Deep Underground Neutrino Experiment (DUNE)

DRAFT Technical Design Report

Volume III:

for CISC TDR development

October 17, 2019

The DUNE Collaboration

DEEP UNDERGROUND NEUTRINO EXPERIMENT

1

Contents

List of Figures

List of Tables

Todo list

reference 1.4 here somewhere or move down 12

Chapter 1

Cryogenics Instrumentation and Slow Controls

1.1 Introduction

The cryogenic instrumentation and slow controls (CISC) consortium provides comprehensive monitoring for all detector components and for liquid argon (LAr) quality and behavior as well as a control system for many detector components. The single-phase (SP) and dual-phase (DP) modules both use the same control system and have nearly identical cryogenic instrumentation except for differences in location due to the different time projection chamber (TPC) geometries and the addition of dedicated instrumentation for monitoring temperature and pressure in the gas phase for the DP module. Volume IV, Dual-Phase Far Detector Module, Chapter 8 of this technical design report (TDR) is virtually the same as this chapter apart from those few differences.

The consortium responsibilities are split into two main branches: cryogenics instrumentation and slow controls, as illustrated in Figure 1.1.

Each element of CISC contributes to the DUNE physics program primarily through the maintenance of high detector live time. As described in Volume II, DUNE Physics, of this TDR, neutrino charge-parity symmetry violation (CPV) and resolution of the neutrino mass hierarchy over the full range of possible neutrino oscillation parameters will require at least a decade of running the far detector (FD). Similar requirements apply to searches for nucleon decay and supernova neutrino burst (SNB) events from within our galaxy. Throughout this long run-time the interior of any DUNE cryostat remains completely inaccessible. No possibility exists for repairs to any components that could be damaged within the TPC structure; hence environmental conditions that present risks must be detected and reported quickly and reliably.

Detector damage risks peak during the initial fill of a module with LAr, as temperature gradients take on their highest values during this phase. Thermal contractions outside of the range of design expectations could result in broken anode plane assembly (APA) wires, silicon photomultipliers

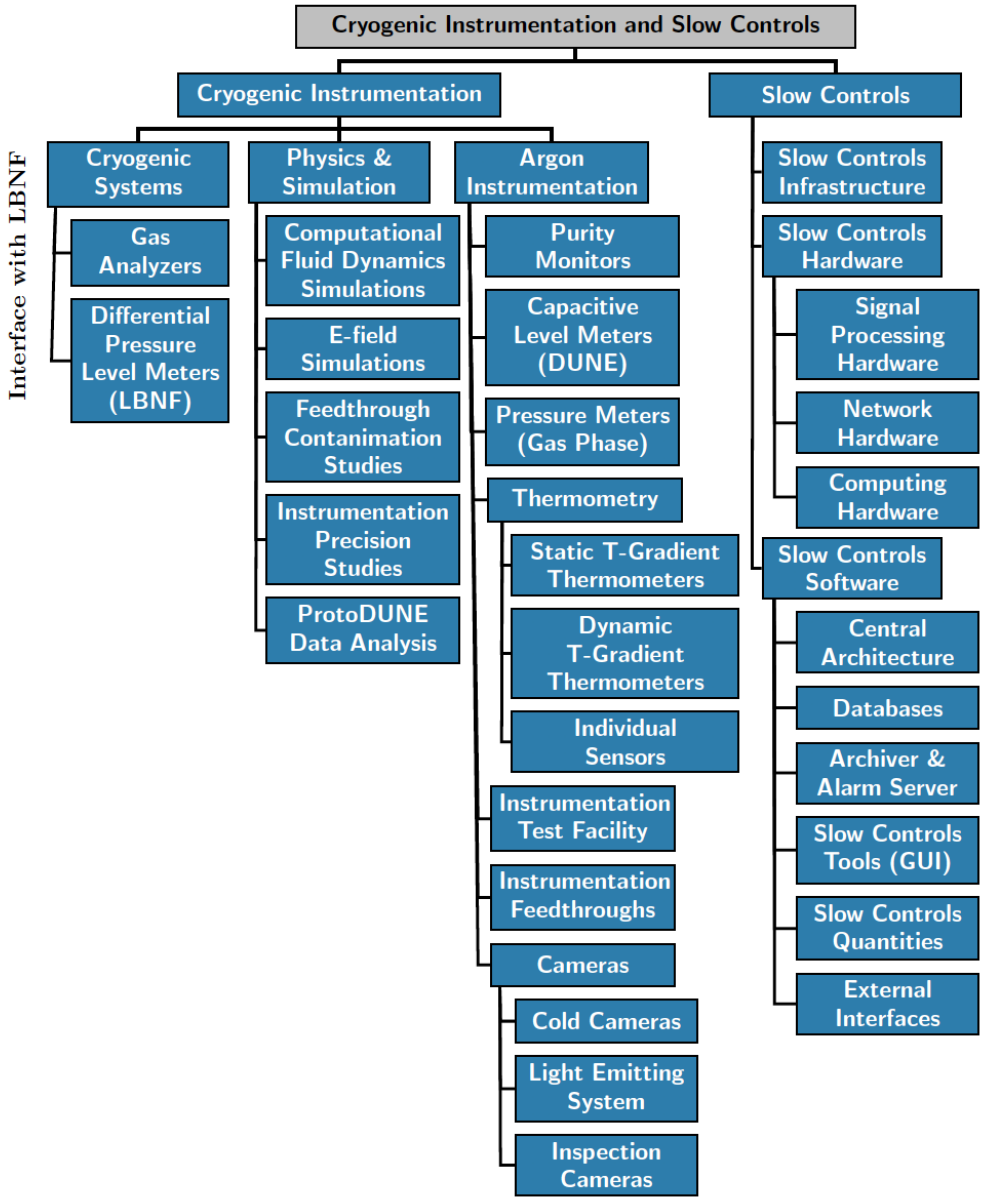

Figure 1.1: CISC subsystem chart

(SiPMs) in photon detectors (PDs) that detach from the X-ARAPUCA light detectors, or poor connections at the cathode high voltage (HV) feedthrough point that could lead to unstable E fields. These considerations lead to the need for a robust temperature monitoring system for the detector, supplemented with liquid level monitors, and a high-performance camera system to enable visual inspection of the interior of the cryostat during the filling process. These systems are fully described in Section 1.2.1 of this chapter.

Argon purity must be established as early as possible in the filling process, a period in which gas analyzers are most useful, and must maintain an acceptable value, corresponding to a minimum electron drift lifetime of 3 ms, throughout the data-taking period. Dedicated purity monitors (Section 1.2.2) provide precise lifetime measurements up to values of 10 ms, the range over which electron attenuation most affects signal-to-noise (S/N) in the TPC. The purity monitors and gas analyzers remain important even after high lifetime has been achieved as periodic detector "top-off" fills occur; the new LAr must be of very high quality as it is introduced into the cryostat.

The CISC system must recognize and prevent fault conditions that could develop in the detector module over long periods of running. For example, the liquid level monitors must register any drop in liquid level; a drop in the level could place top sections of the field cage (FC) or bias HV points for the APAs close enough to the gas-liquid boundary to trigger sparking events. Very slow-developing outgassing phenomena could conceivably occur, with associated bubble generation creating another source of HV breakdown events. The cold camera system enables detection and identification of bubbling sites, and the development of mitigation strategies such as lower HV operation for some period of time. A more subtle possibility is the formation of quasi-stable eddies in argon fluid flow that could prevent positive argon ions from being cleared from the TPC volume, resulting in space charge build up that would not otherwise be expected at the depth of the FD. The space charge could in turn produce distortions in the TPC drift field that degrade tracking and calorimetry performance. The high-performance thermometry of the DUNE CISC system creates input for well developed complex fluid flow models described in Section 1.1.3 that should enable detection of conditions associated with these eddies.

Finally, a high detector live-time fraction over multi-year operation cannot be achieved without an extensive system to monitor all aspects of detector performance, report this information in an intelligent fashion to detector operators, and archive the data for deeper offline studies. Section 1.1.1.2 details the DUNE slow controls system designed for this task.

The baseline designs for all the CISC systems have been used in ProtoDUNE-SP, and most design parameters are extrapolated from these designs. The ProtoDUNE-SP data (and in some cases ProtoDUNE-DP data) will therefore be used to validate the instrumentation designs and to understand their performance.

1.1.1 Scope

1.1.1.1 Cryogenics Instrumentation

Cryogenics instrumentation includes purity monitors, various types of temperature monitors, and cameras with their associated light emitting systems. Also included are gas analyzers and LAr level monitors that are directly related to the external cryogenics system, which have substantial interfaces with the Long-Baseline Neutrino Facility (LBNF). LBNF provides the needed expertise for these systems and is responsible for the design, installation, and commissioning, while the CISC consortium provides the resources and supplements labor as needed.

A cryogenic instrumentation test facility (CITF) for the instrumentation devices is also part of the cryogenics instrumentation. CISC is responsible for design through commissioning in the SP module of LAr instrumentation devices: purity monitors, thermometers, capacitive level meters, cameras, and light-emitting system, and their associated feedthroughs.

Cryogenics instrumentation requires significant engineering, physics, and simulation work, such as E field simulations and cryogenics modeling studies using computational fluid dynamics (CFD). E field simulations identify desirable locations for instrumentation devices in the cryostat, away from regions of high E field, so that their presence does not induce large field distortions. CFD simulations help identify expected temperature, impurity, and velocity flow distributions and guide the placement and distribution of instrumentation devices inside the cryostat.

1.1.1.2 Slow Controls

The slow controls portion of CISC consists of three main components: hardware, infrastructure, and software. The slow controls hardware and infrastructure comprises networking hardware, signal processing hardware, computing hardware, and associated rack infrastructure. The slow controls software provides, for every slow control quantity, the central slow controls processing architecture, databases, alarms, archiving, and control room displays.

CISC provides software and infrastructure for controlling and monitoring all detector elements that provide data on the health of the detector module or conditions important to the experiment, as well as some related hardware.

Slow controls base software and databases are the central tools needed to develop control and monitoring for various detector systems and interfaces. These include:

- base input/output software;
- alarms, archiving, display panels, and similar operator interface tools; and
- slow controls system documentation and operations guidelines.

Slow controls for external systems collect data from systems external to the detector module

and provide status monitoring for operators and archiving. They collect data on beam status, cryogenics status, data acquisition (DAQ) status, facilities systems status, interlock status bit monitoring (but not the actual interlock mechanism), ground impedance monitoring, and possibly building and detector hall monitoring, as needed.

The DUNE detector safety system (DDSS) can provide inputs to CISC on safety interlock status, and CISC will monitor and make that information available to the experiment operators and experts as needed. However, DDSS and CISC are separate monitors, and the slow controls portion of CISC does not provide any inputs to DDSS. A related question is whether CISC can provide software intervention before a hardware safety interlock. In principle such intervention can be implemented in CISC, presumably by (or as specified by) the hardware experts. For example, at ProtoDUNE-SP, the automatic lowering of HV to clear streamers was implemented in the software for the HV control using CISC-level software.

Slow controls covers software interfaces for detector hardware devices, including:

- monitoring and control of all power supplies,
- full rack monitoring (rack fans, thermometers and rack protection system),
- instrumentation and calibration device monitoring (and control to the extent needed),
- power distribution unit and computer hardware monitoring,
- HV system monitoring through cold cameras, and
- detector components inspection using warm cameras.

CISC will develop, install, and commission any hardware related to rack monitoring and control. Most power supplies may only need a cable from the device to an Ethernet switch, but some power supplies might need special cables (e.g., GPIB or RS232) for communication. The CISC consortium is responsible for providing these control cables.

CISC has additional activities outside the scope of the consortium that require coordination with other groups. This is discussed in Section 1.4.4.

1.1.2 Design Considerations

Important design considerations for instrumentation devices include stability, reliability, and longevity, so that devices can survive for at least 20 years. Such longevity is uncommon for any device, so the overall design allows replacement of devices where possible. Some devices are critical for filling and commissioning but less critical for later operations; for these devices we specify a minimum lifetime of 18 months and 20 years as a desirable goal. DUNE requires the E field on any instrumentation devices inside the cryostat to be less than 30 kV/cm to minimize the risk of dielectric breakdown in LAr. A consideration important for event reconstruction is the maximum noise level induced by instrumentation devices that the readout electronics can tolerate. ProtoDUNE-SP is evaluating this. Table 1.1 shows the top-level specifications that determine the requirements for CISC together with selected high-level specifications for CISC subsystems. The physics-driven rationale

for each requirement and the proposed validation are also included in the table. Tables 1.2 and 1.3 show the full set of specifications for the CISC subsystems. In all those tables two values are quoted for most of the design parameters: i) *specification*, which is the intended value or limits for the parameter set by physics and engineering needs, and ii) *goal*, an improved value offering a benefit which the collaboration aims to achieve where it is cost-effective to do so.

Data from purity monitors and different types of thermometers will be used to validate the LAr fluid flow model. A number of requirements drive the design parameters for the precision and granularity of monitor distribution across the cryostat. For example, the electron lifetime measurement precision must be 1.4 % to keep the bias on the charge readout in the TPC below 0.5 % at 3 ms lifetime. For thermometers, the parameters are driven by the CFD simulations based on ProtoDUNE-SP design. The temperature measurement resolution must be less than 2 mK, and the relative precision of those measurements must be less than 5 mK. The resolution is defined as the temperature RMS for individual measurements and is driven by the electronics. The relative precision also includes the effect of reproducibility for successive immersions in LAr. The relative precision is particularly important in order to characterize gradients below 20 mK. As will be described below, the laboratory calibration data and the recent analysis of thermometer instrumentation data from ProtoDUNE-SP shows that a 2.5 mK relative precision is achievable.

The level meters must have a precision of 0.1% over 14 m (i.e., 14 mm) for measurement accuracy during filling. This precision is also sufficient to ensure that the LAr level stays above the ground planes (GPs) of a single-phase (SP) module. As shown in Table 1.3, several requirements drive the design of cold and warm cameras and the associated light emitting system. The components of the camera systems must not contaminate the LAr or produce bubbles so as to avoid increasing the risk of HV discharge. Both cold and warm cameras must provide coverage of at least 80 % of the TPC volume with a resolution of 1 cm for cold cameras and 2 mm for warm cameras on the TPC.

For the CITF, a cryostat with a capacity of only 0.5 to approximately 3 m^3 will suffice and will keep turn-around times and filling costs lower. For gas analyzers, the operating range must allow establishment of useful electron lifetimes; details are in Table 1.2.

For slow controls, the system must be sufficiently robust to monitor a minimum of 150,000 variables per detector module, and support a broad range of monitoring and archiving rates; the estimated variable count, data rate, and archive storage needs are discussed in Section 1.3.4. The system must also interface with a large number of detector subsystems and establish two-way communication with them for control and monitoring. For the alarm rate, 150 alarms/day is used as the specification as it is the maximum to which humans can be expected to respond. The goal for the alarm rate is less than 50 alarms/day. The alarm logic system will need to include features for managing “alarm storms” using alarm group acknowledgment, summaries, delays, and other aids.

Table 1.1: Specifications for SP-CISC ref tab:spec:SP-CISC

Label	Description	Specification (Goal)	Rationale	Validation

SP-FD-5	Liquid argon purity	<100 ppt (<30 ppt)	Provides >5:1 S/N on induction planes for pattern recognition and two-track separation.	Purity monitors and cosmic ray tracks
SP-FD-15	LAr nitrogen contamination	<25 ppm	Maintain 0.5 PE/MeV PDS sensitivity required for triggering proton decay near cathode.	In situ measurment
SP-FD-18	Cryogenic monitoring devices		Constrain uncertainties on detection efficiency, fiducial volume.	ProtoDUNE
SP-FD-25	Non-FE noise contributions	$<<1000\ e^-$	High S/N for high reconstruction efficiency.	Engineering calculation and ProtoDUNE
SP-CISC-1	Noise from Instrumentation devices	$\ll 1000\ e^-$	Max noise for 5:1 S/N for a MIP passing near cathode; per SBND and DUNE CE	ProtoDUNE
SP-CISC-2	Max. E field near instrumentation devices	<30 kV/cm (<15 kV/cm)	Significantly lower than max field of 30 kV/cm per DUNE HV	3D electrostatic simulation
SP-CISC-3	Precision in electron lifetime	$<1.4\%$ ($<1\%$)	Required for accurate charge reconstruction per DUNE-FD Task Force report.	ProtoDUNE-SP and ITF
SP-CISC-4	Range in electron lifetime	0.04 ms to 10 ms in cryostat, 0.04 ms to 30 ms inline	Slightly beyond best values observed so far in other detectors.	ProtoDUNE-SP and ITF
SP-CISC-11	Precision: temperature reproducibility	<5 mK (2 mK)	Enables validation of CFD models, which predicts gradients below 15 mK	ProtoDUNE-SP and ITF
SP-CISC-14	Temperature stability	<2 mK at all places and times (Match precision requirement at all places, at all times)	Measure the temp map with sufficient precision during the entire duration	ProtoDUNE-SP
SP-CISC-27	Cold camera coverage	$>80\%$ of HV surfaces (100%)	Enable detailed inspection of issues near HV surfaces.	Calculated from location, validated in prototypes.
SP-CISC-51	Slow control alarm rate	<150/day (<50/day)	Alarm rate low enough to allow response to every alarm.	Detector module; depends on experimental conditions
SP-CISC-52	Total No. of variables	$>150{,}000$ (150,000 to 200,000)	Scaled from ProtoDUNE-SP	ProtoDUNE-SP
SP-CISC-54	Archiving rate	0.02 Hz (Broad range 1 Hz to 1 per few min.)	Archiving rate different for each variable, optimized to store important information	ProtoDUNE-SP

Table 1.2: List of specifications for the different CISC subsystems

Quantity/Parameter	Specification	Goal
Noise from Instrumentation devices	$\ll$ 1000 enc	
Max. E field near instrumentation devices	$<$30 kV/cm	$<$15 kV/cm
Purity Monitors		
Precision in electron lifetime	$<$1.4% at 3 ms, $<$4% at 9 ms, relative differences $<$2.5%	$<$ 1%
Range in electron lifetime	0.04 - 10 ms	(0.04 - 30 ms inline)
Longevity	20 years	$>$ 20 years
Stability	Match precision requirement at all places/times	
Reliability	Daily Measurements	Measurements as needed
Thermometers		
Vertical density of sensors for T-gradient monitors	$>$ 2 sensor/m	$>$ 4 sensors/m
2D horizontal density for top/bottom individual sensors	1 sensor/5(10) m	1 sensor/3(5) m
Swinging/deflection of T-Gradient monitors	$<$ 5 cm	$<$ 2 cm
Resolution of temperature measurements	$<$ 2 mK	$<$0.5 mK
Precision: temperature reproducibility	$<$ 5 mK	2 mK
Reliability	80% (in 18 months)	50% (during 20 years)
Longevity	$>$ 18 months	$>$ 20 years
Stability	$<$ 2 mK at all places and times	Match precision requirement at all places/times
Discrepancy between lab and in situ calibrations for temperature sensors	$<$ 5 mK	$<$ 3 mK
Discrepancy between measured temperature map and CFD simulations in ProtoDUNE-SP	$<$ 5 mK	
Gas Analyzers		
Operating Range O2	0.2 (air) to 0.1 ppt	
Operating Range H2O	Nom. air to sub ppb; contaminant-dependent	
Operating Range N2	Nominally Air Nom. air to sub ppb; contaminant-dependent	
Precision: 1 sigma at zero	per gas analyzer range	
Detection limit: 3 sigma	Different analyzer modules needed to cover entire range	
Stability	$<$% of full scale range.	
Longevity	$>$10 years	
Pressure Meters (GAr)		
Relative precision (DUNE side)	0.1 mbar	
Absolute precision (DUNE side)	$<$5 mbar	

Table 1.3: List of specifications for the different CISC subsystems

Quantity/Parameter	Specification	Goal
Level Meters		
Precision (LBNF scope)	0.1% over 14 m (14 mm)	
Precision (capacitive level meters, Deep Underground Neutrino Experiment (DUNE) scope)	1 cm	<5 mm
Longevity (all)	20 years	> 20 years
Cold cameras		
Coverage	80% of the exterior of HV surfaces	100%
Frames per second	yet to be defined	
Resolution	1 cm on the TPC	yet to be defined
Duty cycle	yet to be defined	
longevity	> 18 months	> 20 years
Inspection cameras		
Coverage	80% of the TPC	yet to be defined
Frames per second	yet to be defined	
Resolution	2 mm on the TPC	yet to be defined
heat transfer	no generation of bubbles	
longevity	> 18 months	> 20 years
Light emitting system		
radiant flux	> 10 mW/sr	100 mW/sr
power	< 125 mW/LED	
wavelength	red/green	IR/white
longevity	> 18 months (for cold cameras)	> 20 years
cryogenic instrumentation test facility (CITF)		
Dimensions	0.5 to 3 cubic meters	
Temperature stability	±1K	
Turn-Around time	∼9 days	9 days
LAr purity	O2, H2O: low enough to measure drifting electrons of devices under test, ∼ 0.5 ms. N2: ppm for scintillation light tests.	>1.0 ms
Slow Controls		
Alarm rate	<150/day	< 50/day
Total No. of variables per detector module	150,000	150,000 - 200,000
Server rack space	2 racks	3 racks
Archiving rate	0.02 Hz	Broad range 1 Hz to 1 per few min.
Near Detector Status	Beam conditions and detector status	Full beam and detector status

1.1.3 Fluid Dynamics Simulation

Proper placement of purity monitors, thermometers, and liquid level monitors within the detector module requires knowing how LAr flows within the cryostat, given its fluid dynamics, heat and mass transfer, and distribution of impurity concentrations. Fluid flow is also important in understanding how the positive and negative ion excess created by various sources (e.g., ionization from cosmic rays and ^{36}Ar; ion feedback at the liquid-gas interface in a DP detector) is distributed across the detector as it affects E field uniformity. Finally, CFD simulations are crucial to predict the purity of the argon in regions where experimental data is unavailable. The overall goal of the CFD simulations is to better understand and predict the fluid (in either liquid or vapor state) motions and the implications for detector performance.

Fluid motion within the cryostat is driven primarily by small changes in density caused by thermal gradients within the fluid although pump flow rates and inlet and outlet locations also contribute. Heat sources include exterior heat from the surroundings, interior heat from electronics, and heat flow through the pump inlet. In principle, purity monitors can be placed throughout the cryostat to determine if the argon is pure enough for experimentation. However, some areas inside the cryostat are off limits for such monitors.

The fluid flow behavior can be determined by simulating LAr flow within a detector module using Siemens Star-CCM+[1], a commercially available CFD code. Such a model must properly define the fluid characteristics, solid bodies, and fluid-solid interfaces, as well as provide a way to measure contamination, while still maintaining reasonable computation times. In addition, these fluid dynamics simulations can be compared to available experimental data to assess simulation accuracy and credibility.

Although simulation of the detector module presents challenges, acceptable simplifications can accurately represent the fluid, the interfacing solid bodies, and variations of contaminant concentrations. Because of the magnitude of thermal variation within the cryostat, modeling of the LAr is simplified by using constant thermophysical properties, calculating buoyant force with the Boussinesq Model (using a constant density for the fluid with application of a temperature-dependent buoyant force), and a standard shear stress transport turbulence model. Solid bodies that touch the LAr include the cryostat wall, cathode planes, anode planes, GP, and FC. As in previous CFD models of the DUNE 35-ton prototype and ProtoDUNE-SP [2], the FC planes, anode planes, and GP can be represented by porous bodies. Because impurity concentration and electron lifetime do not affect fluid flow, these variables can be simulated as passive scalars, as is commonly done for smoke released [3] in air or dyes released in liquids.

Discrepancies between real data and simulations may affect detector performance. Simulation results contribute to decisions about where to place sensors and monitors and to the definitions of various calibration quantities. Methods of mitigating such risks include well established convergence criteria, sensitivity studies, and comparison to results of previous CFD simulation work. Moreover, the simulation will be improved with input from LAr temperature and purity measurements and validation tests from ProtoDUNE-SP[2].

[1] https://mdx.plm.automation.siemens.com/star-ccm-plus

[2] Because ProtoDUNE-DP was not instrumented with high-precision thermometers in the liquid phase and because

Taking into account that the CFD model can predict both temperature and impurity levels, the procedure for validating and tuning the CFD model will be the following: i) temperature predictions will be constrained with temperature measurements in numerous locations in the cryostat to improve the CFD model, ii) the improved model is then used to predict the LAr impurity level at the location of purity monitors, iii) this prediction is compared with the actual measurement from purity monitors to further constrain the CFD model.

Figure 1.2 shows an example of the temperature distribution on a plane intersecting a LAr inlet and at a plane halfway between an inlet and an outlet; the geometry used for this simulation is shown in Figure 1.3[3]. Note the plume of higher temperature LAr between the walls and the outer APA on the inlet plane. The current placement of instrumentation in the cryostat as shown in Figure 1.5 was determined using temperature and impurity distributions from previous simulations.

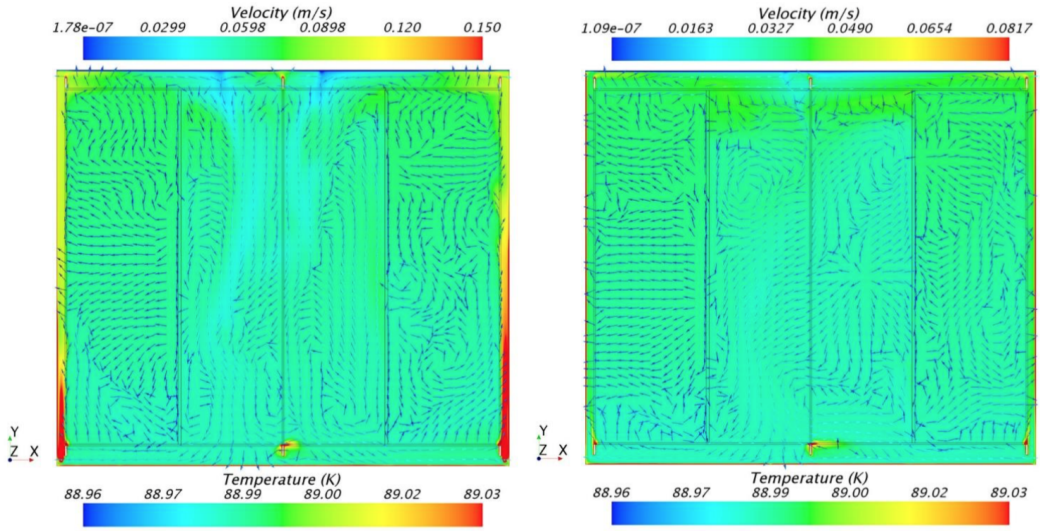

Figure 1.2: Distribution of temperature on a plane intersecting an inlet (left) and halfway between an inlet and an outlet (right), as predicted by previous CFD simulations (from [2]). (See Figure 1.3 for geometry.)

The strategy for future CFD simulations begins with understanding the performance of the ProtoDUNE-SP cryogenics system and modeling the detector modules to derive specifications for instrumentation. We are pursuing a prioritized set of studies to help determine the requirements for other systems. We plan to

- review the DUNE FD cryogenics system design and verify the current implementation in simulation to ensure that the simulation represents the actual design.
- model the ProtoDUNE-SP liquid and gas regions with the same precision as the FD. Presently, we have only the liquid model, which is needed to interpret the thermometer data. The gas model is needed to see how to place thermometers in the ullage and verify the design of the gaseous argon purge system.

the cryogenics design is the same for SP and DP modules of the DUNE FD, ProtoDUNE-SP data will be used to validate the liquid CFD model.

[3]the inlet and outlet map has recently changed; it now consists of two rows of 64 inlets each at each longer side of the cryostat and four outlets along the shorter sides (drift direction) of the cryostat.

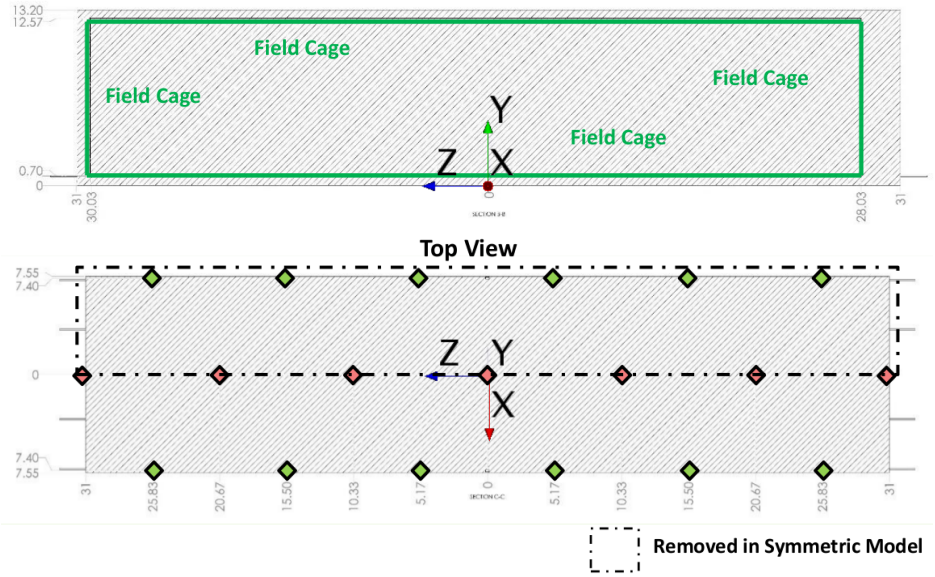

Figure 1.3: Layout of the SP TPC within the cryostat (top) and positions of LAr inlets and outlets (bottom) as modeled in the CFD simulations [2]. The y axis is vertical and the x axis is parallel to the TPC drift direction. Inlets are shown in green and outlets are shown in red.

- verify the CFD model for the SP module in a simulation performed by LBNF; this defines the requirements for instrumentation devices (e.g., thermometry).

reference 1.4 here somewhere or move down

Table 1.4: CFD input parameters for ProtoDUNE-SP

Parameter	Value	Comments
Cryostat height	7.878 m	Measured with laser (1 cm error approx.)
LAr surface height	7.406 m	Measured by capacitive level meter (< 1 cm error)
Ullage pressure	1.045 bar	Measured by pressure gauges
LAr surface temperature	87.596 K	Computed using ullage pressure and [4]
LAr inlet temperature	bulk LAr + 0.2 K	Estimated from pressure settings in cryo-system
LAr flow rate per pipe	0.417 kg/s	Estimated from cryostat filling rate

1.1.3.1 Validation in ProtoDUNE

ProtoDUNE-SP has collected data to validate the CFD using:

- static and dynamic T-gradient thermometers,
- individual temperature sensors placed in the return LAr inlets,

- two 2D grids of individual temperature sensors installed below the bottom ground planes and above the top ground planes,
- a string of three purity monitors vertically spaced from near the bottom of the cryostat to just below the LAr surface,
- two pressure sensors (relative and absolute) in the argon gas,
- H_2O, N_2, and O_2 gas analyzers,
- LAr level monitors, and
- standard cryogenic sensors including pressure transducers, individual temperature sensors placed around the cryostat on the membrane walls, and recirculation flow rates transducers.

The data, which has been logged through the ProtoDUNE-SP slow control system [5], is available for offline analysis.

In parallel, CISC has produced a ProtoDUNE-SP CFD model with input from ProtoDUNE-SP measurements (see Table 1.4). Streamlines[4] from the current simulation (Figure 1.4) show the flow paths from the four cryostat inlets to the outlet. The validation of this model consists of an iterative process in which several versions of the CFD simulation, using different input parameters, eventually converge to a reasonable agreement with data from instrumentation devices. Those comparisons will be shown in Section 1.2.1.4

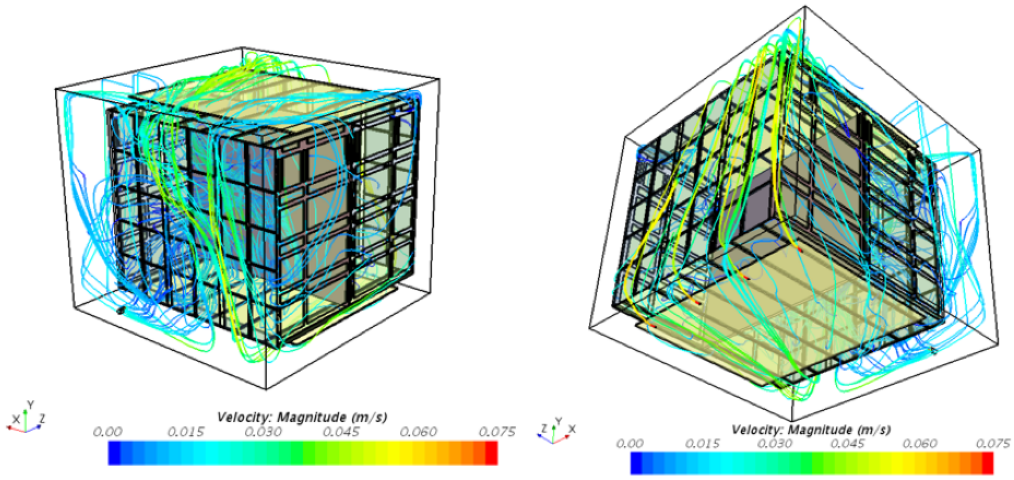

Figure 1.4: Streamlines for LAr flow inside ProtoDUNE-SP

Once the ProtoDUNE-SP CFD model predicts the fluid temperature in the entire cryostat to a reasonable level under different conditions, we will use it to produce maps of impurity levels in the detector module. These can be easily converted into electron lifetime maps, which we will compare to the ProtoDUNE-SP purity monitor data.

[4] In fluid mechanics, a streamline is a line that is everywhere tangent to the local velocity vector. For steady flows, a streamline also represents the path that a single particle of the fluid will take from inlet to exit.

1.2 Cryogenic Instrumentation

Instrumentation inside the cryostat must accurately report the condition of the LAr so that we can ensure that it is adequate to operate the TPC. This instrumentation includes purity monitors to check the level of impurity in the argon and to provide high-precision electron lifetime measurements, as well as gas analyzers to verify that the levels of atmospheric contamination do not rise above certain limits during the cryostat purging, cooling, and filling. Temperature sensors deployed in vertical arrays and at the top and bottom of the detector module monitor the cryogenics system operation, providing a detailed 3D temperature map that helps predict the LAr purity across the entire cryostat. The cryogenics instrumentation also includes LAr level monitors and a system of internal cameras to help find sparks in the cryostat and to monitor the overall cryostat interior.

The proper placement of purity monitors, thermometers, and liquid-level monitors in the detector module requires understanding the LAr fluid dynamics, heat and mass transfer, and the distribution of impurity concentrations within the cryostat. Both this and coherent analysis of the instrumentation data require CFD simulation results.

ProtoDUNE-SP is testing the performance of purity monitors, thermometers, level monitors and cameras for the SP module, validating the baseline design.

1.2.1 Thermometers

As discussed in Section 1.1.3, a detailed 3D temperature map is important for monitoring the cryogenic system for correct functioning and the LAr for uniformity. Given the complexity and size of purity monitors, they can only be installed on the sides of the cryostat to provide a local measurement of LAr purity. A direct measurement of the LAr purity across the entire cryostat is not feasible, but a sufficiently detailed 3D temperature map based on CFD simulations can predict it. The vertical coordinate is especially important because it will relate closely to the LAr recirculation and uniformity.

The baseline sensor distribution and the cryostat ports used to extract cables (with indication of number of cables per port) are shown in Figure 1.5. The baseline distribution will evolve as more information becomes available (precise CFD simulations, better understanding of detector support system (DSS) ports, installation interfaces with other groups), but the baseline suffices to establish the overall strategy.

High-precision temperature sensors will be distributed near the TPC walls in two ways: (1) forming high density (> 2 sensors/m) vertical arrays (called T-gradient monitors) and (2) in coarser (~ 1 sensor/5 m) 2D arrays (called individual sensors) at the top and bottom of the detector module, where it is most crucial to know the temperature.

Expected temperature variations inside the cryostat are very small (0.02 K; see Figure 1.2), so sensors must be cross-calibrated to better than 0.005 K. Most sensors will be calibrated in the

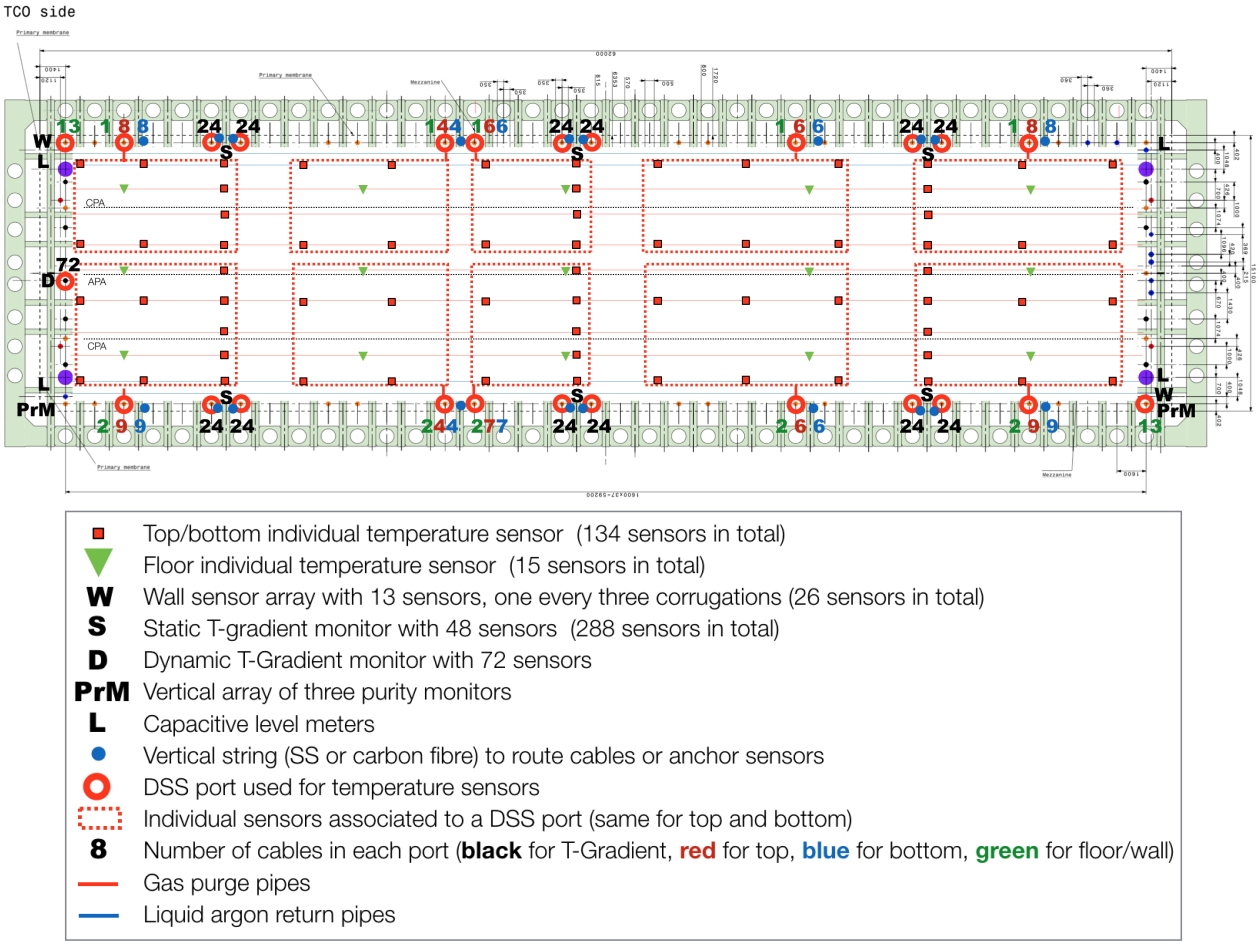

Figure 1.5: Distribution of temperature sensors inside the cryostat

laboratory before installation (installation is described in Section 1.4.5.2). Calibration before installation is the only option for sensors installed on the long sides of the detector and the top and bottom of the cryostat, where space is limited. Given the precision required and the unknown longevity of the sensors – possibly requiring another calibration after some time – an additional method will be used for T-gradient monitors installed on the short ends of the detector in the space between the field cage end walls and the cryostat walls. There is sufficient space in this area for a movable system, which can be used to cross calibrate the temperature sensors *in situ*, as described in 1.2.1.1.

The baseline design for all thermometer systems have three elements in common: sensors, cables, and readout system. We plan to use Lake Shore PT100-series[5] platinum sensors with 100 Ω resistance because in the temperature range 83 K to 92 K they show high reproducibility of ∼ 5 mK and absolute temperature accuracy of 100 mK. Using a four-wire readout greatly reduces issues related to lead resistance, any parasitic resistances, connections through the flange, and general electromagnetic noise pick-up. Lakeshore PT102 sensors (see Figure 1.13, right) were used in the 35 ton prototype and ProtoDUNE-SP, giving excellent results. For the inner readout cables, a custom cable made by Axon[6] is the baseline. It consists of four teflon-jacketed copper wires (American wire gauge (AWG) 28), forming two twisted pairs, with a metallic external shield and an outer teflon jacket. The readout system is described in Section 1.2.1.5.

Another set of lower-precision sensors epoxied into the bottom membrane of the cryostat will monitor the cryostat filling in the initial stage. Finally, the inner walls and roof of the cryostat will have the same types of sensors to monitor the temperature during cooldown and filling ("W" sensors in Figure 1.5).

1.2.1.1 Dynamic T-gradient monitors

To address concerns about potential differences in sensor readings prior to and after installation in a detector module, and potential drifts over the lifetime of the module that may affect accuracy of the vertical temperature gradient measurement, a dynamic temperature monitor allows cross-calibration of sensor readings in situ. Namely, this T-gradient monitor is motorized, allowing vertical motion of the temperature sensor array in the detector module, enabling precise cross-calibration between the sensors, as illustrated in Figure 1.6.

The procedure for cross-calibrations is the following: in step 1, the temperature reading of all sensors is taken at the home (lowest) position of the carrier rod. In step 2, the stepper motor moves the carrier rod up 25 cm. Since the sensors along the entire carrier rod are positioned 25 cm apart, when the system is moved up 25 cm, each sensor is positioned at the height that was occupied by another sensor in step 1. Then a second temperature reading is taken. In this manner, except for the lowest position two temperature measurements are taken at each location with different sensors. Assuming that the temperature at each location is stable over the few minutes required to make the measurements, any difference in the temperature readings between the two different sensors is due to their relative measurement offset. This difference

[5] Lake Shore Cryotronics™ platinum RTD series, `https://www.lakeshore.com/`.
[6] Axon™ Cable, `http://www.axon-cable.com`.

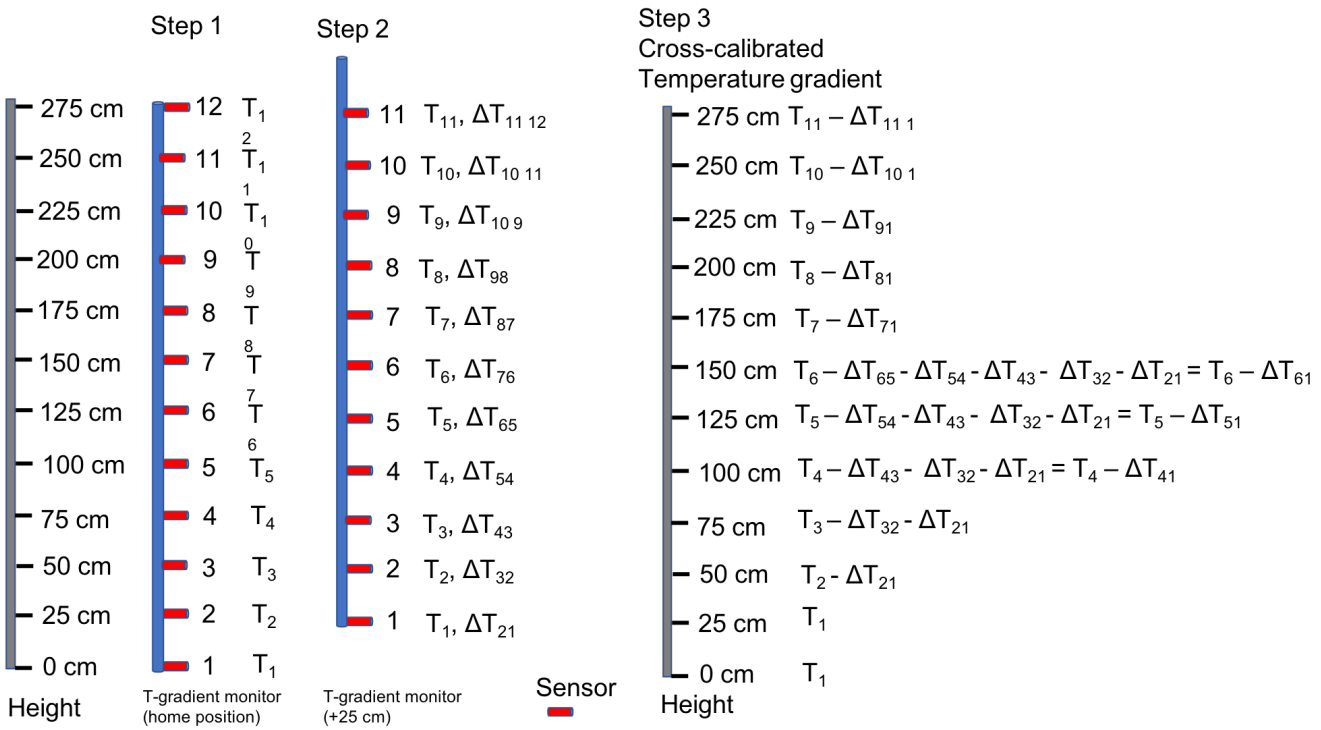

Figure 1.6: In step 1, sensor temperature measurements are taken with the T-gradient monitor in the home position. In step 2, the entire system is moved up 25 cm and another set of temperature readings is taken by all sensors. Then, the offsets between pairs of sensors are calculated for each position. In step 3, offsets are linked together, providing cross-calibration of all sensors, to obtain the entire vertical temperature gradient measurement with respect to a single sensor (number 1 in this case).

is then calculated for all locations. In step 3, readout differences between pairs of sensors at each location are linked to one another, expressing temperature measurements at all heights with respect to a single sensor. In this way, temperature readings from all sensors are cross-calibrated in situ, canceling all possible offsets due to electromagnetic noise or any parasitic resistances that may have prevailed despite the four-point connection to the sensors that should cancel most of the offsets. These measurements are taken with a very stable current source, which ensures high precision of repeated temperature measurements over time. The motion of the dynamic T-monitor is stepper-motor operated, delivering measurements with high spatial resolution.

A total of 72 sensors will be installed with 25 cm spacing, decreased to 10 cm spacing for the top and bottom 1 m of the carrier rod. The vertical displacement of the system is such that every sensor can be moved to the nominal position of at least five other sensors, minimizing the risks associated with sensor failure and allowing for several points of comparison. The total expected motion range of the carrier rod is 1.35 m.

This procedure was tested in ProtoDUNE-SP, where the system was successfully moved up by a maximum of 51 cm, allowing cross-calibration of all sensors (22 sensors with 10.2 cm spacing at top and bottom and 51 cm in the middle).

Figure 1.7 shows the temperature profile after calibration when the recirculation pumps are off. Under these conditions the temperature should be very homogeneous except near the surface. This is indeed what is observed in that figure, demonstrating the reliability of the method.

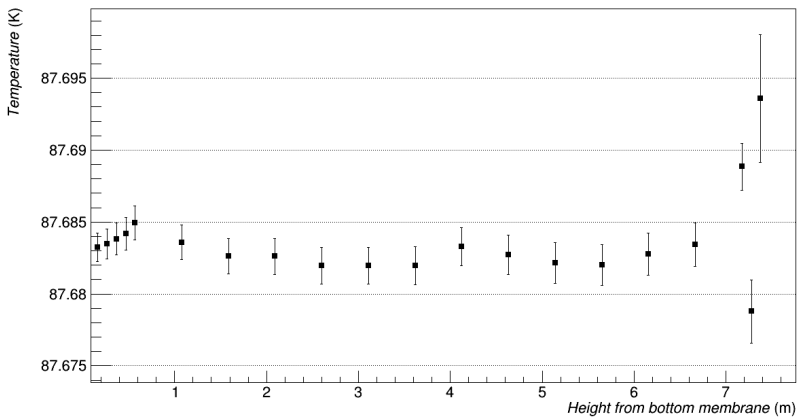

Figure 1.7: Temperature profile as measured by the dynamic T-gradient monitor after cross-calibration, when the recirculation pumps are off. Temperature variation is of the order of 3 mK except close to the top and the gas phase interface, as expected.

A dynamic T-gradient monitor has three parts: a carrier rod on which sensors are mounted; an enclosure above the cryostat housing space that allows the carrier rod to move vertically 1.5 m over its lowest location; and the motion mechanism. The motion mechanism consists of a stepper motor connected through a ferrofluidic dynamic seal to a gear and pinion motion mechanism. The sensors have two pins soldered to a printed circuit board (PCB). Two wires are individually soldered to the common soldering pad for each pin. A cutout in the PCB around the sensor allows free flow of argon for more accurate temperature readings. Stepper motors typically have very fine steps that allow highly precise positioning of the sensors. Figure 1.8 shows the overall design of the dynamic T-gradient monitor. The enclosure has two parts connected by a six-cross flange. One

side of this flange will be used for signal wires, another will be used as a viewing window, and the two other ports will be spares. Figure 1.9, left shows the PCB mounted on the carrier rod and the sensor mounted on the PCB along with the four point connection to the signal readout wires. Figure 1.9, right shows the stepper motor mounted on the side of the rod enclosure. The motor remains outside the enclosure, at room temperature, as do its power and control cables.

Figure 1.8: A schematic of the dynamic T-gradient monitor.

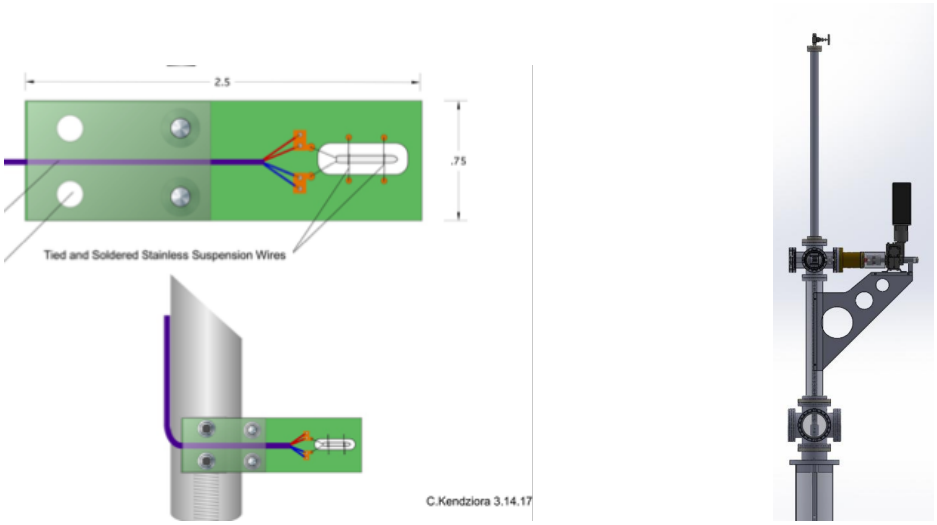

Figure 1.9: Left: Sensor mounted on a PCB board and PCB board mounted on the rod. Right: The driving mechanism of the dynamic T-gradient monitor, consisting of a stepper motor driving the pinion and gear linear motion mechanism.

1.2.1.2 Static T-gradient monitors

Several vertical arrays of high-precision temperature sensors cross-calibrated in the laboratory will be installed behind the APAs. The baseline design assumes six arrays with 48 sensors each. Spacing between sensors is 20 cm at the top and bottom and 40 cm in the middle area. This configuration is similar to the one used in ProtoDUNE-SP but with nearly double the spacing. As shown in Figure 1.10 a configuration with 48 sensors was appropriate in ProtoDUNE-SP, as it should be in the SP module where the expected total gradient is no larger than in ProtoDUNE-SP (see Figure 1.2).

Sensors will be cross-calibrated in the laboratory using a controlled environment and a high-precision readout system, described in Section 1.2.1.5. The accuracy of the calibration for ProtoDUNE-SP was estimated to be 2.6 mK, as shown in Figure 1.11. Preliminary results for the analysis of ProtoDUNE-SP static T-gradient monitor data are shown in Figure 1.10. The temperature profile has been computed using both the laboratory calibration and the so-called *in-situ pump-off calibration*, which consists of estimating the offsets between sensors assuming the temperature of LAr in the cryostat is homogeneous when the re-circulation pumps are off (the validity of this method

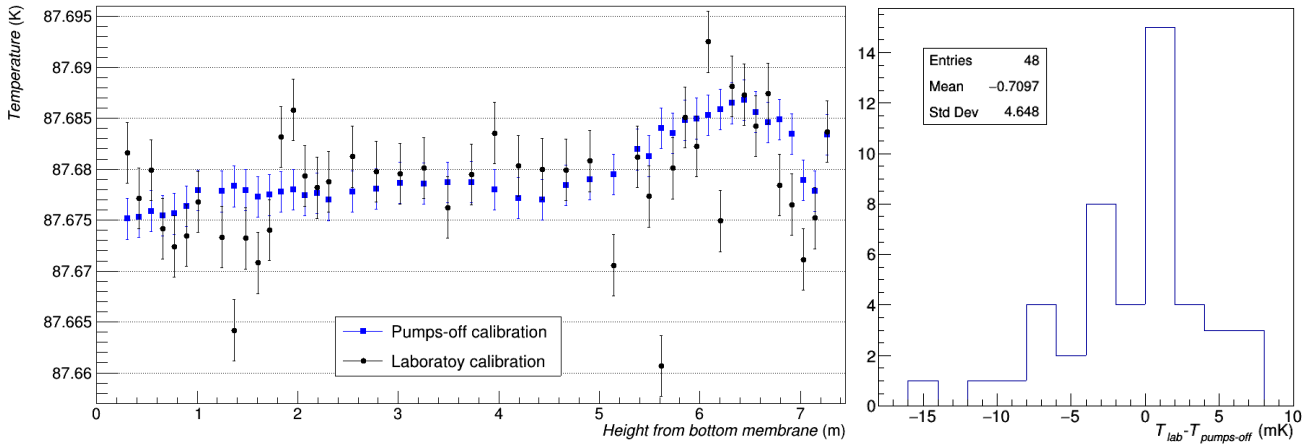

Figure 1.10: Left: Temperature profile as measured by the static T-gradient monitor for two different calibration methods. Right: Distribution of the difference between both methods.

is demonstrated in Section 1.2.1.1). The RMS of the difference between both methods is 4.6 mK, slightly larger than the value quoted above for the accuracy of the laboratory calibration, due to the presence of few outliers (under investigation) and to the imperfect assumption of homogeneous temperature when pumps are off (see Figure 1.7).

Figure 1.12 shows the baseline mechanical design of the static T-gradient monitor. Two strings (stainless steel or carbon fibre) are anchored at the top and bottom corners of the cryostat using the available M10 bolts (see Figure 1.13, left). One string routes the cables while the other supports the temperature sensors. Given the height of the cryostat, an intermediate anchoring point to reduce swinging is under consideration. A prototype is being built at IFIC, Spain, where the full system will be mounted using two dummy cryostat corners.

Figure 1.13 (right) shows the baseline design of the ($52 \times 15\,\mathrm{mm}^2$) PCB support for temperature sensors with an IDC-4 male connector. A narrower connector (with two rows of two pins each) is being studied. This alternative design would reduce the width of the PCB assembly and allow more sensors to be calibrated simultaneously. Each four-wire cable from the sensor to the flange will have an IDC-4 female connector on the sensor end; the flange end of the cable will be soldered or crimped to the appropriate connector, whose type and number of pins depend on the final design of the DSS ports that will be used to extract the cables. SUBD-25 connectors were used in ProtoDUNE-SP.

1.2.1.3 Individual Temperature Sensors

T-gradient monitors will be complemented by a coarser 2D array (every 5 m) of precision sensors at the top and bottom of the detector module, as shown in Figure 1.5. Following the ProtoDUNE-SP design, bottom sensors will use the cryogenic pipes as a support structure, while top sensors will be anchored to the GPs. Although sensors at the top will have a similar distribution to those at the bottom, suitable anchoring points at the top and bottom will differ.

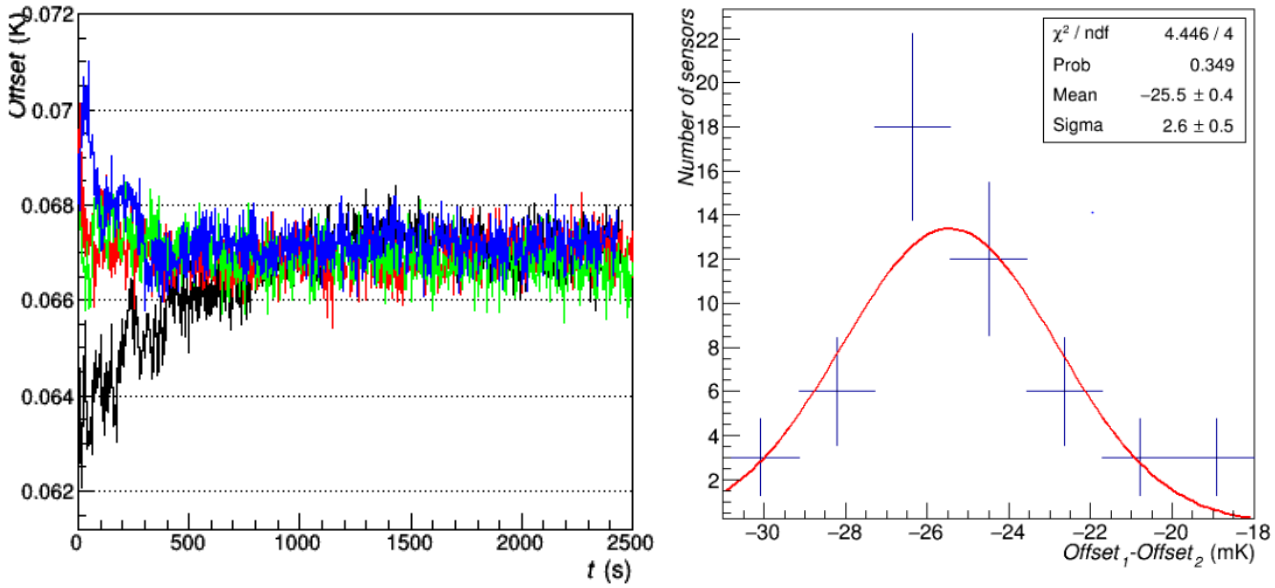

Figure 1.11: Left: Temperature offset between two sensors as a function of time for four independent immersions in LAr. The reproducibility of those sensors, defined as the RMS of the mean offset in the flat region, is $\sim$ 1 mK, The resolution for individual measurements, defined as the RMS of one offset in the flat region, is better than 0.5 mK. Right: Difference between the mean offset obtained with two independent calibration methods for the 51 calibrated sensors. The standard deviation of this distribution is interpreted as precision of the calibration.

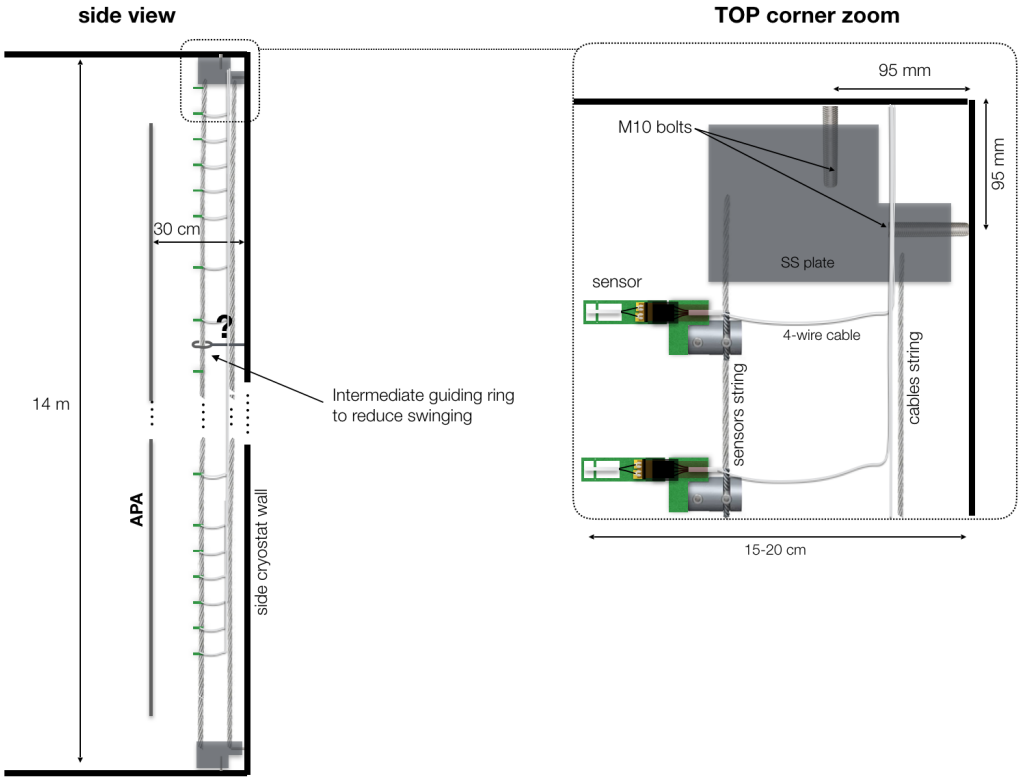

Figure 1.12: Conceptual design of the static T-gradient monitor.

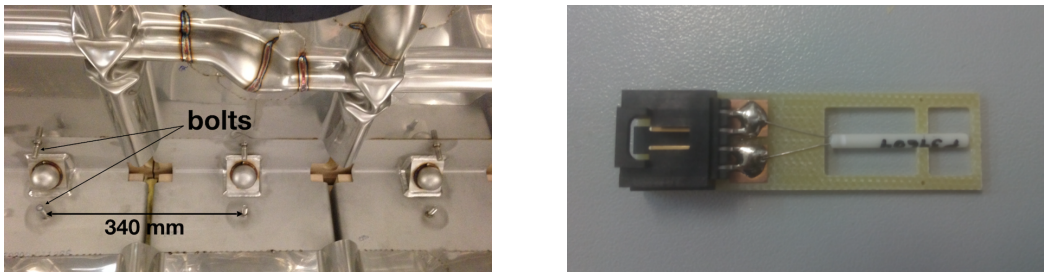

Figure 1.13: Left: bolts at the bottom corner of the cryostat. Right: Lakeshore PT102 sensor mounted on a PCB with an IDC-4 connector.

As in ProtoDUNE-SP, another set of standard sensors will be evenly distributed and epoxied to the bottom membrane. They will detect the presence of LAr when cryostat filling starts. Finally, two vertical arrays of standard sensors will be epoxied to the lateral walls in two opposite vertical corners, with a spacing of 102 cm (every three corrugations), to monitor the cryostat membrane temperature during the cooldown and filling processes.

Whereas in ProtoDUNE-SP cables were routed individually (without touching neighboring cables or any metallic elements) to prevent grounding loops in case the outer Teflon jacket broke, such a failure has been proved to be very unlikely. Thus, in the detector modules, cables will be routed in bundles, simplifying the design enormously. As Figure 1.5 shows, up to 20 sensors will use the same DSS port, large enough for a cable bundle 16 mm in diameter.

Cable bundles of several sizes will be configured using custom made Teflon pieces that will be anchored to different cryostat and detector elements to route cables from sensors to DSS ports. For sensors at the bottom (on pipes and floor), cables will be routed towards the cryostat bottom horizontal corner using stainless steel split clamps anchored to pipes (successfully prototyped in ProtoDUNE-SP), and from there, to the top of the cryostat using vertical strings (as with static T-gradient monitors). For sensors on the top GPs, cables bundles will be routed to the corresponding DSS port using Teflon supports attached to both the FR-4 threaded rods in the union between two GP modules and to the DSS I-beams (both successfully prototyped in ProtoDUNE-SP). Sensors on the walls will use bolts in the vertical corners for cable routing.

For all individual sensors, PCB sensor support, cables, and connection to the flanges will be the same as for the T-gradient monitors.

1.2.1.4 Analysis of temperature data in ProtoDUNE-SP

Temperature data from ProtoDUNE-SP has been recorded since LAr filling in August 2018. The analysis of this data and the comparison with CFD simulations is actively underway, but interesting preliminary results are available and will be described below. Figure 1.14 shows the distribution of temperature sensors in the ProtoDUNE-SP cryostat.

All precision temperature sensors (for the static and dynamic T-gradient monitors, and the 2D arrays at top and bottom) were calibrated in the laboratory prior to installation. However, since the

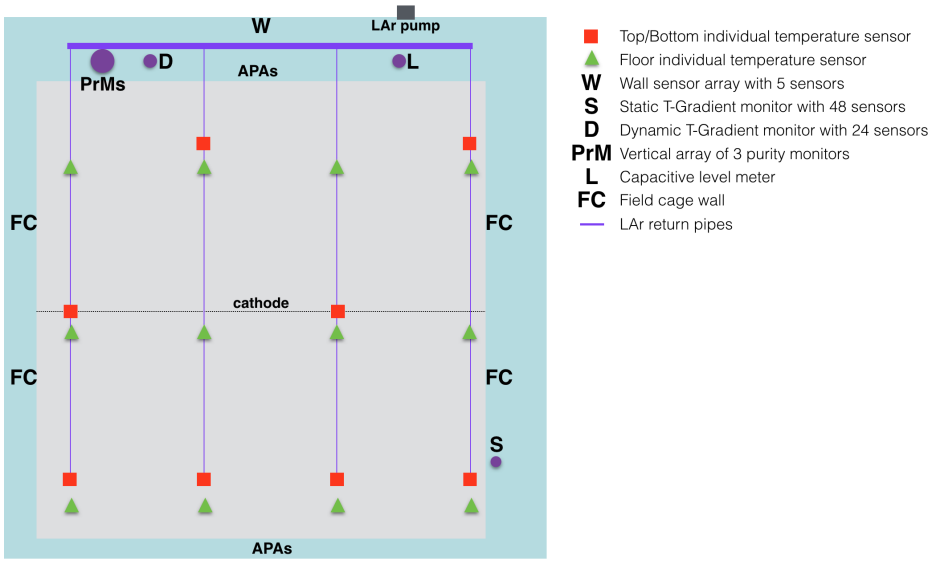

Figure 1.14: Distribution of temperature sensors in the ProtoDUNE-SP cryostat. Notice that four of the bottom sensors are located right above the LAr inlets. Purity monitors and level meters are also indicated.

calibration method was still under development when those sensors were installed, this calibration was only satisfactory (2.6 mK precision) for the static T-gradient monitor, whose sensors were calibrated the last and plugged in just few days prior to installation in the cryostat. In Section 1.2.1.2, an additional calibration method, the so called *pumps-off calibration*, has been described and the agreement with the laboratory calibration was proved (see Figure 1.10). Since this is the only reliable calibration for individual sensors, this method will be used for the data analysis presented in this section, for all sensors except for the dynamic T-gradient monitor, whose calibration based on the movable system is more precise (see Section 1.2.1.1).

Figure 1.15 shows the vertical temperature profiles as measured by the dynamic and static T-gradient monitors at a given moment in time (10 minutes in May 2019). The stability of those profiles has been carefully studied: the relative variation between any two sensors on the same profiler is below 3 mK along the entire data taking, probing that the shape of the profiles is nearly constant in time. In Figure 1.15 one immediately observes that the shapes of the two profiles are similar, with a bump at 6.2 m, but the magnitude of variation of the static profile almost doubles compared to the dynamic profile. This effect is attributed to the fact that the dynamic T-gradient monitor is on the path of the LAr flow, which makes the temperature more uniform, while the static profiler is on the side.

In order to connect the two different regions covered by the T-gradient monitors, temperature measurements by the bottom sensor grid can be used. Figure 1.16 shows the temperature difference between bottom sensors and the second sensor of the static T-gradient monitor (the one at 40 cm from the floor), which is used as reference. Also shown in the figure is the third sensor of the dynamic T-gradient monitor, located at a similar height. Three different periods are shown in the figure: two periods with pumps-on and one period with pumps-off. It is observed that when the pumps are working the temperature decreases towards the LAr pump, being higher in the sensors below the cathode. The horizontal gradient observed in this situation is of the order of 20 mK

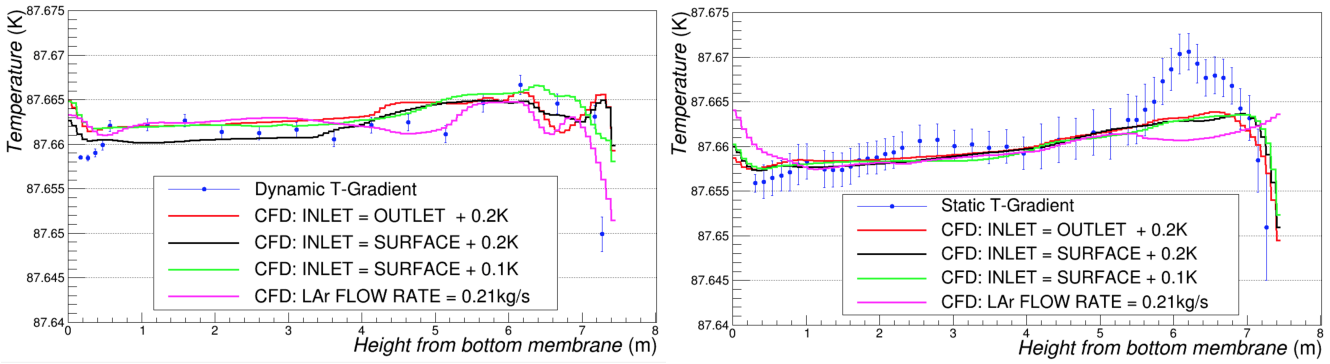

Figure 1.15: Temperature profiles measured by the T-gradient monitors and comparison to the CFD model with different boundary conditions. Left: dynamic T-gradient monitor; Right: Static T-gradient monitor.

– larger than the vertical gradient. When the pumps are off the horizontal gradient decreases, although a residual gradient of 5 mk is observed. This gradient is attributed to the inertia of the liquid once the pumps are switched off: it takes more than one day to recover the horizontal homogeneity.

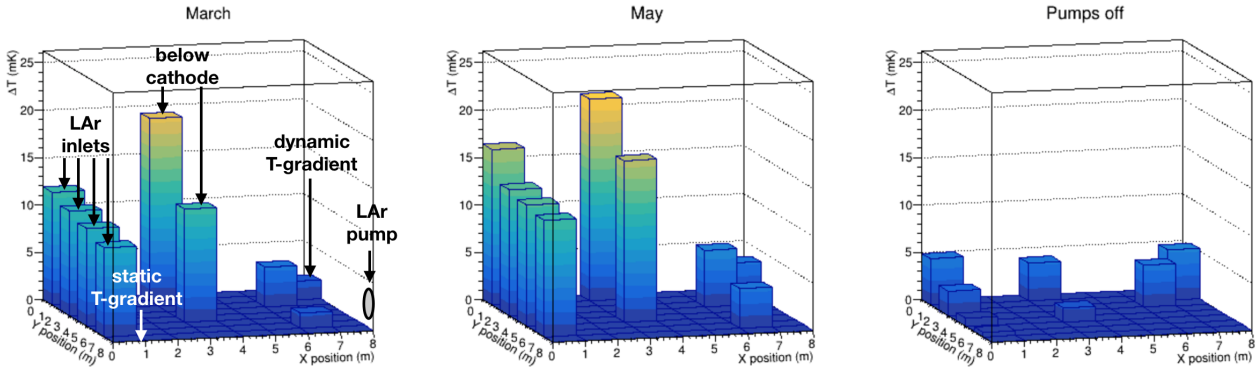

Figure 1.16: Temperature difference between bottom sensors at 40 cm from the floor and static T-gradient sensor at same height. The third dynamic T-gradient sensor, which is at the same height, is also shown. Two pumps-on periods (left and middle panels) and one pump-off period (right panel) are shown.

CFD simulations have been produced with different inputs. Two parameters have been identified as potential drivers of the convection regime: i) the incoming LAr flow rate and ii) the incoming LAr temperature. The result of varying those parameters was shown in Figure 1.15. The CFD model reasonably predicts the main features of the data but the details still need to be understood: the bump at 6.2 m or the lower measured temperature at the bottom. It is worth noting that the simulation depends minimally on the LAr temperature while the flow rate has more impact, specially in the regions where discrepancies are larger. All simulations use the nominal LAr flow rate, 0.42 kg/s, except the one explicitly indicated in the plots, which uses half of the rate. More simulations with other LAr flow rates are needed to conclude.

The CFD reassuringly predicts a reasonable response for more than one set of initial conditions. It is still important to instrumentation response to help establish the validity of the CFD model.

We did not run tests with differing initial conditions during the beam run because even controlled changes of the cryostat environment could have undesirable effects. However, dedicated tests to validate the CFD under various deliberate changes of the cryostat were performed recently. Those additional tests include pump and recirculation manipulations such as pump on-off, change of pumping speed, and bypassing of filtration, and changing the cryostat pressure set point to a higher (or lower) value[7] to induce changes in the pressure for a specified time while monitoring the instrumentation. Any change in pressure could change the temperatures everywhere in the cryostat. Studying the rate of this change, as detected at various heights in the cryostat, might provide interesting constraints on the CFD model.

1.2.1.4.1 Comparison of calibration methods

Three different calibration methods have been described above, each of them having a different purpose. The underlying assumption is that reliable temperature monitoring at the few mK level is desirable during the entire lifetime of the experiment, both to guarantee the correct functioning of the cryogenics system and to compute offline corrections based on temperature measurements and CFD simulations. This is only possible if an insitu calibration method is available since relative calibration between sensors is expected to diverge with time with respect to the one performed in the laboratory. Two insitu methods have been used. The pumps-off calibration method is very powerful since it is the only way of cross-calibrating all sensors in the cryostat at any point in time. However it relies on the assumption that the temperature is uniform when the recirculation pumps are off. The validity of this assumption has to be bench-marked with real data and this is done in ProtoDUNE-SP using the calibration based on the movable system (see Fig 1.7). The last is the most precise calibration method and the one that sustains all other methods, providing a reliable reference during the entire lifetime of the experiment. This method is even more crucial for the far detector. Indeed, recirculation pumps will be located on one side of the cryostat, very far (almost 60 m) from some regions of the LAr volume, where the inertia will be more pronounced and the homogeneous temperature assumption becomes less valid.

1.2.1.5 Readout system for thermometers

A high-precision and very stable system is required to achieve a readout level of < 5 mK. The proposed readout system was used in ProtoDUNE-SP and relies on a variant of an existing mass PT100 temperature readout system developed at CERN for an LHC experiment; it has already been tested and validated in ProtoDUNE-SP. The system has an electronic circuit that includes

- a precise and accurate current source[8] for the excitation of the temperature sensors measured using the four-wires method,

[7] The HV was ramped down for this exercise because dropping the pressure too fast might provoke boiling of the LAr near the surface.

[8] The actual current delivered is monitored with high precision resistors such that the effect of ambient temperature can be disentangled.

- a multiplexing circuit connecting the temperature sensor signals and forwarding the selected signal to a single line, and
- a readout system with a high-accuracy voltage signal readout module[9] with 24 bit resolution over a 1 V range.

This readout system also drives the multiplexing circuit and calculates temperature values. The CompactRIO device is connected to the detector Ethernet network, sending temperature values to the DCS software through a standard OPC UA driver.

The current mode of operation averages more than 2000 samples taken every second for each sensor. Figure 1.11 shows the system has a resolution higher than 1 mK, the RMS of one of the offsets in the stable region.

1.2.2 Purity Monitors

A fundamental requirement of a LAr TPC is that ionization electrons drift over long distances in LAr. Part of the charge is inevitably lost due to electronegative impurities in the liquid. To keep this loss to a minimum, monitoring impurities and purifying the LAr during operation is essential.

A purity monitor is a small ionization chamber used to infer independently the effective free electron lifetime in the LArTPC. It illuminates a cathode with UV light to generate a known electron current, then collects the drifted current at an anode a known distance away. Attenuation of the current is related to the electron lifetime. Electron loss can be parameterized as $N(t) = N(0)e^{-t/\tau}$, where $N(0)$ is the number of electrons generated by ionization, $N(t)$ is the number of electrons after drift time t, and τ is the electron lifetime.

For the SP module, the drift distance is 3.5 m, and the E field is $500\,\mathrm{V}\cdot\mathrm{cm}^{-1}$. Given the drift velocity of approximately $1.5\,\mathrm{mm}\cdot\mu\mathrm{s}^{-1}$ in this field, the time to go from cathode to anode is roughly $\sim$2.4 ms [6]. The LAr TPC signal attenuation, $[N(0) - N(t)]/N(0)$, must remain less than 20 % over the entire drift distance [7]. The corresponding electron lifetime is $2.4\,\mathrm{ms}/[-\ln(0.8)] \simeq 11\,\mathrm{ms}$.

Residual gas analyzers can be used to monitor the gas in the ullage of the tank and would be an obvious choice for analyzing argon gas. Unfortunately, suitable and commercially available mass spectrometers have a detection limit of $\sim$10 parts per billion (ppb), whereas DUNE requires a sensitivity of parts per trillion (ppt). Therefore, specially constructed and distributed purity monitors will measure LAr purity in all phases of operation. These measurements, along with an accurate CFD model, enable the determination of purity at all positions throughout the detector module.

The large scale of the DUNE detector modules increases the risk of failing to notice unexpected cryogenic and circulation failures. If these conditions were to persist, it could cause irreversible contamination to the LAr and terminate useful data taking. Well scheduled purity monitor runs can catch sudden drops in e-lifetime, therefore mitigate this risk, as demonstrated in ProtoDUNE-

[9] National Instrument CompactRIO™ device with a signal readout NI9238™ module.

SP. Purity monitors' role to mitigate this risk is unique because the cosmic-ray rate in DUNE's deep-underground FD is too low for TPC to measure e-lifetime frequently with its data.

Purity monitors are placed inside the cryostat but outside of the TPC. They are also placed within the recirculation system outside the cryostat, both in front of and behind the filtration system. Continuous monitoring of the LAr supply lines to the detector module provides a strong line of defense against contamination from sources both in the LAr volume and from components in the recirculation system. Similarly, gas analyzers (described in Section 1.2.5) protect against contaminated gas.

Furthermore, using several purity monitors to measure lifetime with high precision at carefully chosen points provides key input, e.g., vertical gradients in impurity concentrations, for CFD models of the detector module.

Purity monitors were deployed in previous liquid argon time-projection chamber (LArTPC) experiments, e.g., ICARUS, MicroBooNE, and the 35 ton prototype. During the first run of the 35 ton prototype, two of the four purity monitors stopped working during cooldown, and a third operated intermittently. We later found that this was due to poor electrical contacts between the resistor chain and the purity monitor. A new design was implemented and successfully tested in the second run.

ProtoDUNE-SP and ProtoDUNE-DP use purity monitors to measure electron lifetime at different heights.

Figure 1.17 shows the assembly of the ProtoDUNE-SP purity monitors. The design reflects improvements to ensure electric connectivity and improve signals. ProtoDUNE-SP uses a string of purity monitors connected with stainless steel tubes to protect the optic fibers.

ProtoDUNE-SP implements three purity monitors. The purity monitors continuously monitored LAr purity during all commissioning, beam test and operation periods of ProtoDUNE-SP. Figure 1.18 shows the ProtoDUNE-SP data taken using its three purity monitors from commissioning of ProtoDUNE-SP starting in September 2018, through the entire beam running, to July 2019.

Although ProtoDUNE-SP receives ample cosmic ray data to perform electron lifetime measurements, the purity monitor system was found to be essential for providing quick, reliable real-time monitoring of purity in the detector and to catch purity related changes in time due to liquid argon recirculation issues. The purity monitor system at ProtoDUNE-SP measured electron lifetime every hour during commissioning and daily during the beam test. During this time, it alerted the experiment to serious problems several times. The first time was for filter saturation during LAr filling, and the rest were recirculation pump stoppages, false alarms, and problems from the cryostat-level gauges. The dips in Figure 1.18 show these sudden changes in purity caught by purity monitors. The purity alerts made by purity monitors prevented situations which otherwise would have continued unnoticed for some time, with serious consequences to the ability to take any data.

Each purity monitor e-lifetime measurement is based on purity monitor anode-to-cathode signal ratios from 200 UV flashes within 40 seconds at the same location, and the statistical error on the

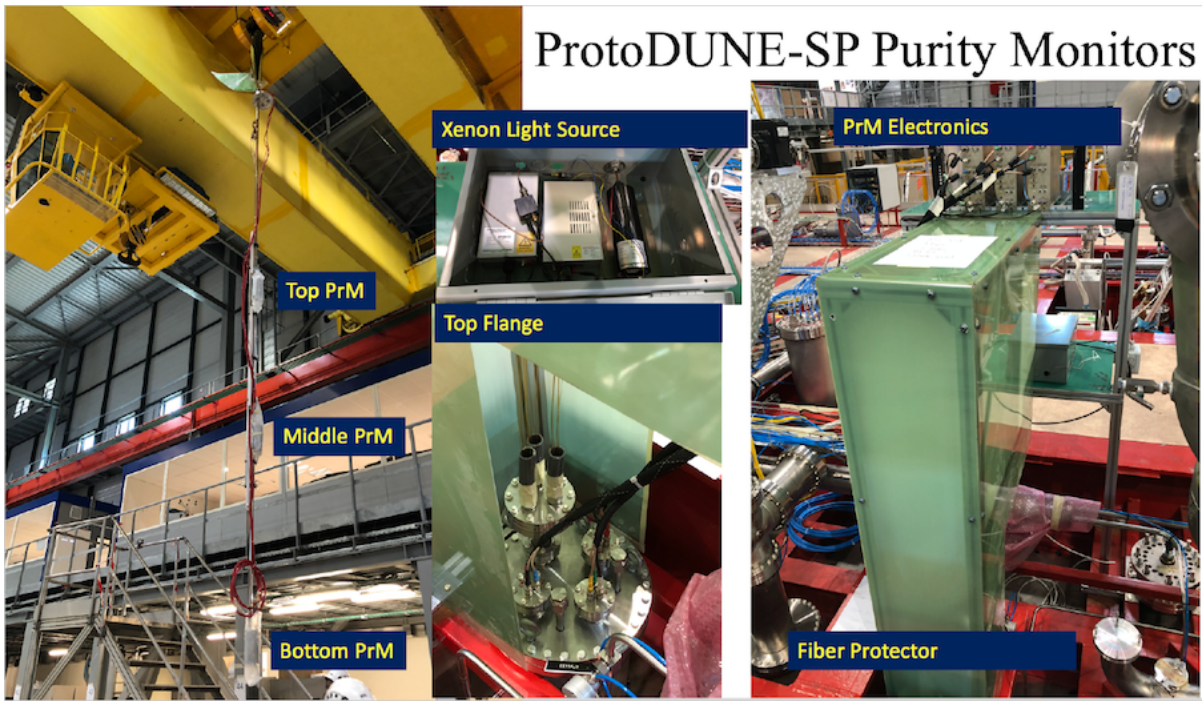

Figure 1.17: The ProtoDUNE-SP purity monitoring system

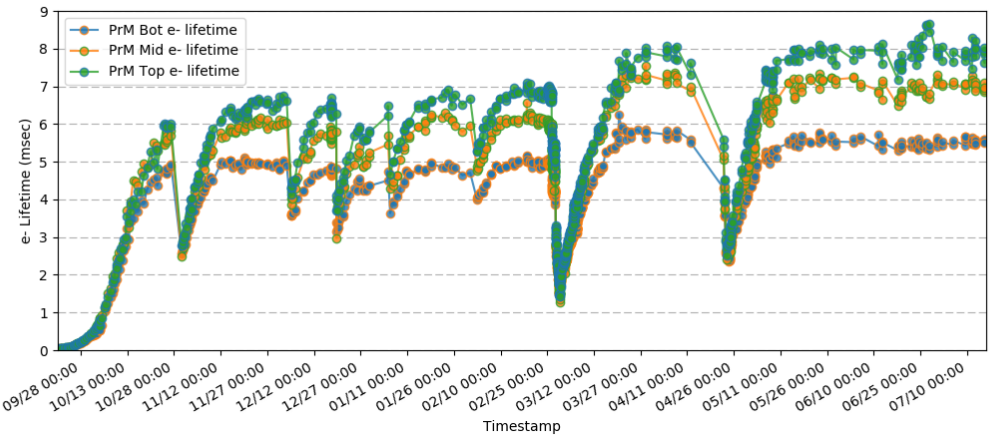

Figure 1.18: The electron lifetimes measured by three purity monitors in ProtoDUNE-SP as a function of time, September 2018 through July 2019. The purity is low prior to start of circulation in October. Reasons for later dips include recirculation studies and recirculation pump stoppages.

purity monitor e-lifetime is less than 0.03 ms when the purity is 6 ms. With this high sensitivity, purity monitors caught the purity drops immediately and make the alert to the experiment in time.

During the commissioning and beam test of ProtoDUNE-SP, the purity monitors operated with different high voltages to change electron drift time, ranging from 150 µs to 3 ms. This allowed the ProtoDUNE-SP purity monitors to measure electron lifetime from 35 µs to about 10 ms with high precision, a dynamic range greater than 300. This measurement was also valuable for the ProtoDUNE-SP lifetime calibration. Because purity monitors have much smaller drift volumes than the TPC, they are less affected by the space charge caused by cosmic rays.

A similar purity monitoring system design and operation plan is planned for the SP module, with modifications to accommodate the relative positions of the instrumentation port and the purity monitor system, and the different geometric relationships between the TPC and cryostat.

1.2.2.1 Purity Monitor Design

The SP module baseline purity monitor design follows that of the ICARUS experiment (Figure 1.19)[8]. It consists of a double-gridded ion chamber immersed in the LAr volume with four parallel, circular electrodes, a disk holding a photocathode, two grid rings (anode and cathode), and an anode disk. The cathode grid is held at ground potential. The cathode, anode grid, and anode each hold separate bias voltages and are electrically accessible via modified vacuum-grade HV feedthroughs. The anode grid and the field shaping rings are connected to the cathode grid by an internal chain of 50 MΩ resistors to ensure the uniformity of the E fields in the drift regions. A stainless mesh cylinder is used as a Faraday cage to isolate the purity monitor from external electrostatic background.

The purity monitor measures the electron drift lifetime between its anode and cathode. The purity monitor's UV-illuminated photocathode generates the electrons via the photoelectric effect. Because the electron lifetime in LAr is inversely proportional to the electronegative impurity concentration, the fraction of electrons generated at the cathode that arrives at the anode (Q_A/Q_C) after the electron drift time t gives a measure of the electron lifetime τ: $Q_A/Q_C \sim e^{-t/\tau}$.

Once the electron lifetime becomes much larger than the drift time t the purity monitor reaches its sensitivity limit. For $\tau >> t$, the anode-to-cathode charge ratio becomes ~ 1. Because the drift time is inversely proportional to the E field, in principle, lowering the field should make it possible to measure lifetimes of any length, regardless of the length of the purity monitor. On the other hand, increasing the voltage will shorten the drift time, allowing measurement of a short lifetime when purity is low.

The electron lifetime of the purest commercial LAr, after the first filtering and during the filling process, is typically higher than 40 µs. However, when the filter starts to saturate, the lifetime decreases to less than 30 µs. To reduce the energy loss due to impurities, the SP module requires an electron lifetime greater than 3 ms.

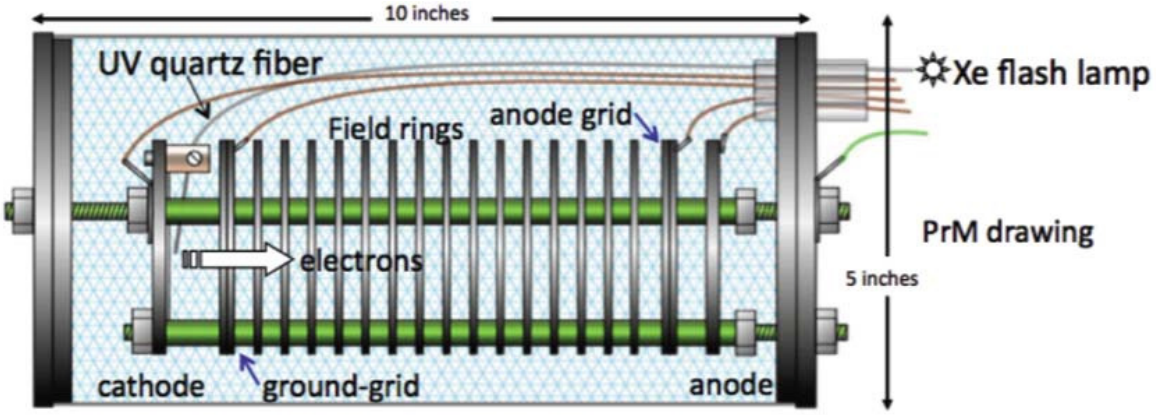

Figure 1.19: Schematic diagram of the basic purity monitor design [8].

Varying the operational HV on the anode from 250 V to 4000 V in the ProtoDUNE-SP's 24 cm (9.5 inch) long purity monitor allowed us to make the 35 µs to 10 ms electron lifetime measurements. Purity monitors with different lengths (drift distances) are needed to extend the measurable range to below 35 µs and above 10 ms.

The photocathode that produces the photoelectrons is an aluminum plate coated first with 50 Å of titanium followed by 1000 Å of gold, and is attached to the cathode disk. A xenon flash lamp is the light source in the baseline design, although a more reliable and possibly submersible light source, perhaps LED-driven, could replace this in the future. The UV output of the lamp is quite good, approximately $\lambda = 225$ nm, which corresponds closely to the work function of gold (4.9 eV to 5.1 eV). Several UV quartz fibers carry the xenon UV light into the cryostat to illuminate the photocathode. Another quartz fiber delivers the light into a properly biased photodiode outside the cryostat to provide the trigger signal when the lamp flashes.

1.2.2.2 Electronics, DAQ, and Slow Controls Interfacing

The purity monitor electronics and DAQ system consist of front-end (FE) electronics, waveform digitizers, and a DAQ PC. Figure 1.20 illustrates the system.

The baseline design of the FE electronics follows that used in the 35 ton prototype, LAPD, and MicroBooNE. The cathode and anode signals are fed into two charge amplifiers contained within the purity monitor electronics module. This electronics module includes a HV filter circuit and an amplifier circuit, both shielded by copper plates, to allow the signal and HV to be carried on the same cable and decoupled inside the purity monitor electronics module. A waveform digitizer that interfaces with a DAQ PC records the amplified anode and cathode outputs. The signal and HV cable shields connect to the grounding points of the cryostat and are separated from the electronic ground with a resistor and a capacitor connected in parallel, mitigating ground loops between the cryostat and the electronics racks. Amplified output is transmitted to an AlazarTech ATS310 waveform digitizer[10] containing two input channels, each with 12 bit resolution. Each channel can

[10] AlazarTech ATS310™ - 12 bit, 20 MS/s, https://www.alazartech.com/Product/ATS310.

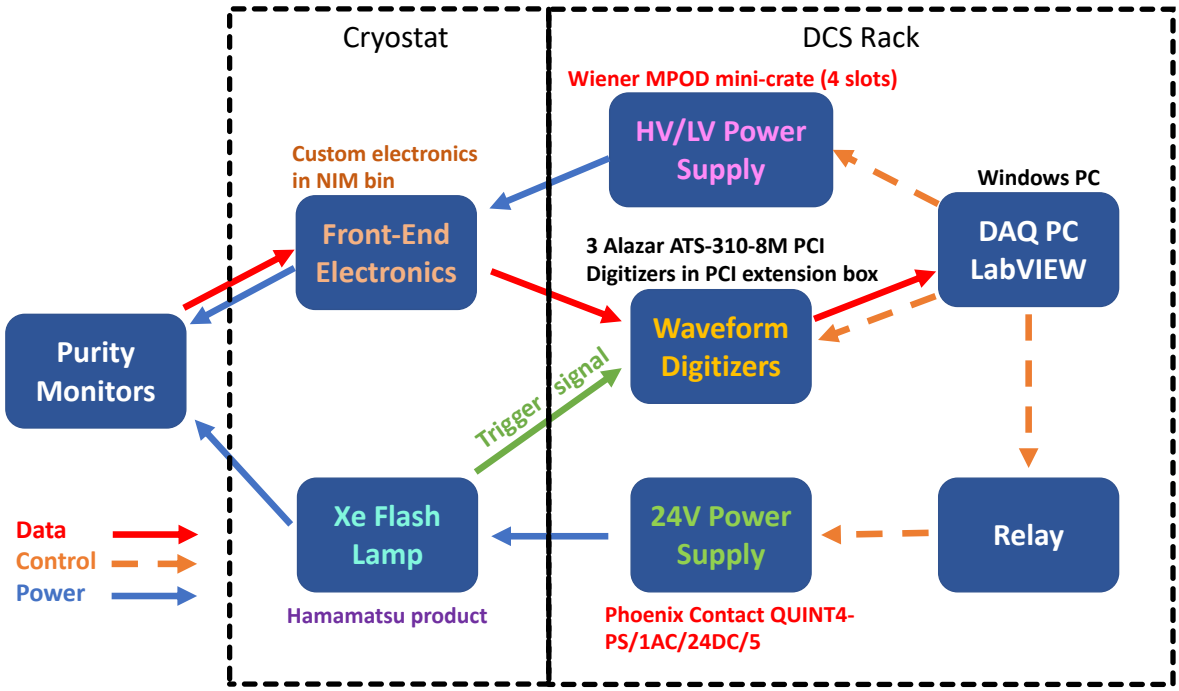

Figure 1.20: Block diagram of the purity monitor system.

sample a signal at a rate of $20\,\mathrm{MS}\cdot\mathrm{s}^{-1}$ to $1\,\mathrm{kS}\cdot\mathrm{s}^{-1}$ and store up to 8 MS in memory. One digitizer is used for each purity monitor, and each digitizer interfaces with the DAQ PC across the PCI bus.

A custom LabVIEW[11] application running on the DAQ PC has two functions: it controls the waveform digitizers and the power supplies, and it monitors the signals and key parameters. The application configures the digitizers to set the sampling rate, the number of waveforms to be stored in memory, the pre-trigger data, and a trigger mode. A signal from a photodiode triggered by the xenon flash lamp is fed directly into the digitizer as an external trigger to initiate data acquisition. LabVIEW automatically turns on the xenon flash lamp by powering a relay when data taking begins and then turns it off when finished. The waveforms stored in the digitizers are transferred to the DAQ PC and used to obtain averaged waveforms to reduce the electronic noise in them. The baseline is estimated by averaging the waveform samples prior to the trigger. This baseline is subtracted from the waveforms prior to calculating peak voltages of the cathode and anode signals. The application performs these processes in real time. The application continuously displays the waveforms and important parameters like measured electron lifetime, peak voltages, and drift time in the purity monitors, and shows the variation in these parameters over time, thus pointing out effects that might otherwise be missed. Instead of storing the measured parameters, the waveforms and the digitizer configurations are recorded in binary form for offline analysis. HV modules[12] in a WIENER MPOD mini crate[13] supply negative voltages to the cathode and positive voltages to the anode. The LabVIEW application controls and monitors the HV systems through an Ethernet interface.

[11] National Instruments, LabVIEW™, http://www.ni.com/en-us.html
[12] iseg Spezialelektronik GmbH™ high voltage supply systems, https://iseg-hv.com/en.
[13] W-IE-NE-R MPOD™ Universal Low and High Voltage Power Supply System, http://www.wiener-d.com/.

The xenon flash lamp and the FE electronics are installed close to the purity monitor flange, to reduce light loss through the optical fiber and prevent signal loss. Other pieces of equipment that distribute power to these items and collect data from the electronics are mounted in a rack separate from the cryostat. The slow control system communicates with the purity monitor DAQ software and controls the HV and LV power supplies of the purity monitor system. The optical fiber must be placed within 0.5 mm of the photocathode for efficient photoelectron extraction, so little interference with the photon detection system (PD system) is expected. The purity monitors could induce noise in the TPC electronics, in particular via the current surge through a xenon lamp when it is flashed. This source of noise can be controlled by placing the lamp inside its own Faraday cage with proper grounding and shielding. At ProtoDUNE-SP, after careful checks of the grounding, this noise has remained well below the noise generated by other sources.

In the SP module we can make use of triggering to prevent any potential noise from the purity monitor's flash lamp from affecting TPC and PD system signals. The LArTPC trigger rate is a few hertz, and each trigger window is one or a few milliseconds. The pulse from a flash lamp is very short (a microsecond or so, much shorter than the gaps between LArTPC trigger windows). Thus, a LArTPC trigger signal may be sent to a programmable pulse generator, which generates a trigger pulse that does not overlap with LArTPC trigger windows. This trigger pulse is then sent to the external trigger port on the flash lamp HV controller so that the lamp flashes between LArTPC trigger windows. In this way, the electronic and light noises from the flash lamp do not affect data taking at all.

1.2.2.3 Production and Assembly

The CISC consortium will produce the individual purity monitors, test them in a test stand, and confirm that each monitor operates at the required level before assembling them into the strings of three monitors each that will be mounted in the detector module cryostat using support tubes. The assembly process will follow the methodology developed for ProtoDUNE.

A short version of the string with all purity monitors will be tested at the CITF. The full string will be assembled and shipped to SURF. A vacuum test in a long vacuum tube will be performed on-site before inserting the full assembly into the SP module cryostat.

1.2.3 Liquid Level Meters

The goals for the LAr level monitoring system are basic level sensing when filling, and precise level sensing during static operations.

Filling the cryostat with LAr will take several months. During this operation several systems will be use to monitor the LAr level. The first 5.5 m will be covered by cameras and by the vertical arrays of Resistance temperature detectors (RTDs) at known heights, since temperature will change drastically when the cold liquid reaches each RTD. Once the liquid reaches the level of the cryogenic pipes going out of the cryostat, the differential pressure between that point and the

bottom of the cryostat can be converted to depth using the known density of LAr. Fine tuning of the final LAr level will be done using several capacitive level meters at the top of the cryostat.

During operation, liquid level monitoring has two purposes: the LBNF cryogenics system uses monitoring to tune the LAr flow, and DUNE uses monitoring to guarantee that the top GPs are always submerged at least 20 cm below the LAr surface to mitigate the risk of dielectric breakdown. This was the value used for the HV interlock in ProtoDUNE-SP.

The LAr flow is tuned using two differential pressure level meters, installed as part of the cryogenics system, one on each side of the detector module. They have a precision of 0.1 %, which corresponds to 14 mm at the nominal LAr surface. Cryogenic pressure sensors will be purchased from commercial sources. Installation methods and positions will be determined as part of the cryogenics internal piping plan.

For HV integrity, multiple 4 m long capacitive level sensors (with a precision of less than 5 mm) will be deployed along the top of the fluid for use during stable operations, and checked against each other. One capacitive level sensor at each of the four corners of the cryostat will provide sufficient redundancy to ensure that no single point of failure compromises the measurement.

Figure 1.21 shows the evolution of the ProtoDUNE-SP LAr level over two months as measured by the differential pressure and capacitive level meters.

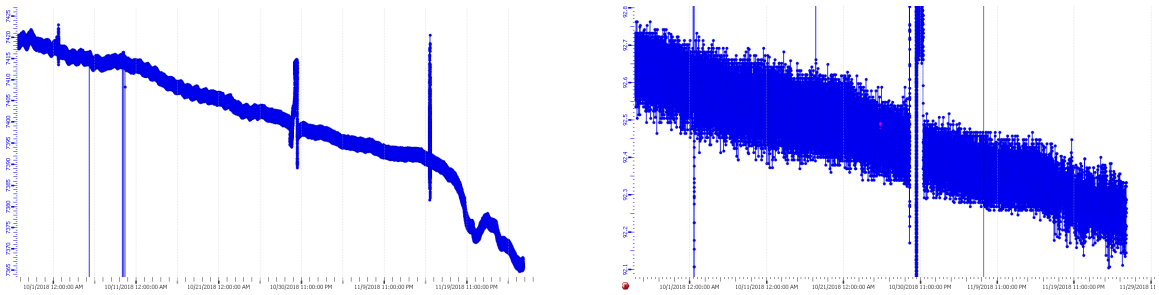

Figure 1.21: Evolution of the ProtoDUNE-SP LAr level over two months. Left: Measured by the capacitive level meter. Right: Measured by the differential pressure level meter. The units in the vertical axis are percentages of the cryostat height (7878 mm).

ProtoDUNE-SP is using the same design for differential pressure level meters which will also be used in the far detector SP module. In the case of capacitive level meters, ProtoDUNE-SP is using commercially bought 1.5 m long level meters while ProtoDUNE-DP is using 4 m long level meters that are custom-built by CERN. For the DUNE FD, we plan to use the longer capacitive level meters custom-built by CERN for both SP and DP modules.

1.2.4 Pressure Meters

The absolute temperature in the liquid varies with the pressure in the argon gas, therefore, precise measurements of pressure inside the cryostat allows for a better understanding of temperature gradients and CFD simulations. In ProtoDUNE, pressure values were also be used to understand

the strain gauge signals installed in the cryostat frame.

Standard industrial pressure sensors can be used to measure the pressure of the argon gas in the ullage in the cryostat. For the DUNE FD, the plan is to follow the same design and configuration used in ProtoDUNE-SP. ProtoDUNE uses two types of pressure sensors and a pressure switch as described below:

- A relative pressure sensor (range: 0-400 mbar, precision: 0.01 mbar),
- An absolute pressure sensor (range: 0-1600 mbar, precision: 0.05 mbar),
- A mechanical relative pressure switch adjustable from 50 to 250 mbar.

Both sensors and the pressure switch are installed in a dedicated flange as shown in figure 1.22 and are connected directly to a slow controls system programmable logic control (PLC) circuit. Dedicated analog inputs are used to read the current values (4 to 20 mA) which are then converted to pressure according to the sensors range. Given the much larger size of DUNE FD, the system described above will be doubled for redundancy: two flanges in opposite cryostat sides will be instrumented with three sensors each.

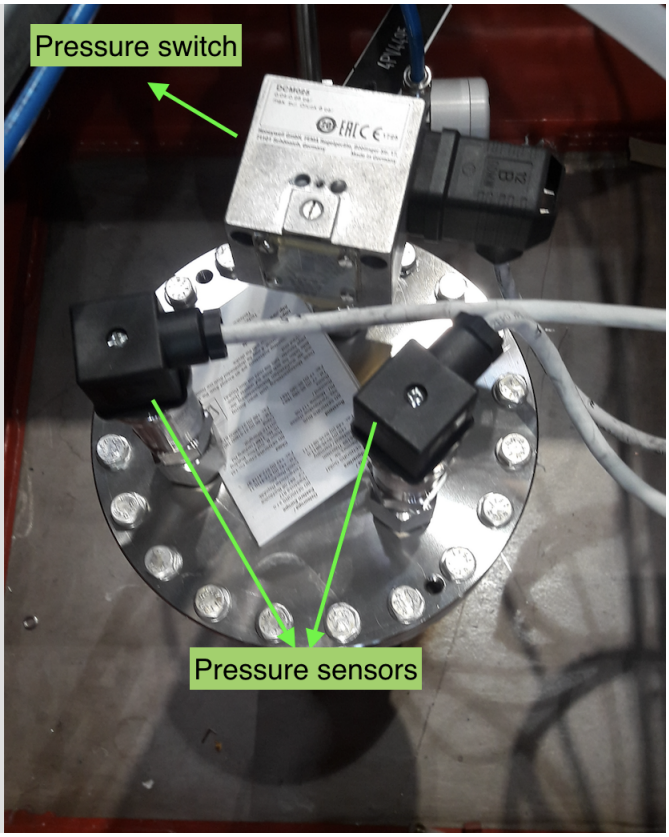

Figure 1.22: Photograph of the pressure sensors installed on a flange in ProtoDUNE-SP.

There are also relative and absolute pressure sensors (with comparatively lower precision) installed by LBNF which are also recorded by the slow controls system. The availability of two types of sensors from LBNF and CISC allows for redundancy, independent measurements, and cross checks.

1.2.5 Gas Analyzers

Gas analyzers are commercially produced modules that measure trace quantities of specific gases contained within a stream of carrier gas. The carrier gas for DUNE is argon, and the trace gases of interest are oxygen (O_2), water (H_2O), and nitrogen (N_2). O_2 and H_2O affect the electron lifetime in LAr and must be kept below 0.1 ppb (O_2 equivalent) while N_2 affects the efficiency of scintillation light production at levels higher than 1 ppm. The argon is sampled from either the argon vapor in the ullage or from the LAr by using small diameter tubing run from the sampling point to the gas analyzer. Typically, the tubing from the sampling points are connected to a switchyard valve assembly used to route the sample points to the desired gas analyzers (see Figure 1.23).

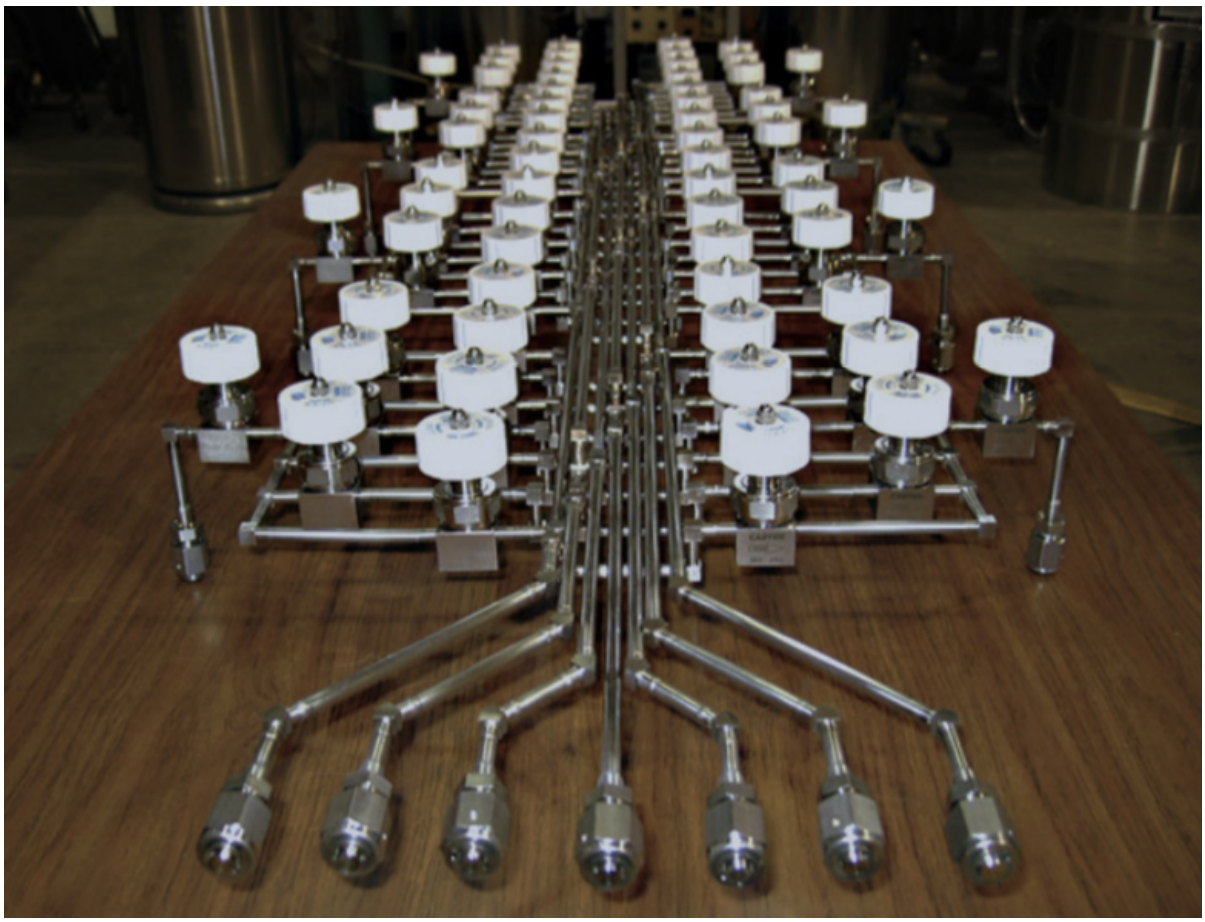

Figure 1.23: A gas analyzer switchyard that routes sample points to the different gas analyzers.

The gas analyzer would be predominantly used during three periods:

1. Once the detector is installed and after the air atmosphere is eliminated from the cryostat to levels low enough to begin cooldown. This purge and gas recirculation process is detailed in Section 1.4.5.3. Figure 1.24 shows the evolution of the N_2, O_2, and H_2O levels from gas analyzer data taken during the purge and recirculation stages of the DUNE 35 ton prototype phase 1 run.

2. Before other means of monitoring impurity levels (e.g., purity monitors, or TPC tracks) are

sensitive, to track trace O_2 and H_2O contaminants from tens of ppb to hundreds of ppt. Figure 1.25 shows an example plot of O_2 levels at the beginning of LAr purification from one of the later 35 ton prototype HV runs.

3. During cryostat filling to monitor the tanker LAr delivery purity. This tracks the impurity load on the filtration system and rejects any deliveries that do not meet specifications. Specifications for the delivered LAr are in the 10 ppm range per contaminant.

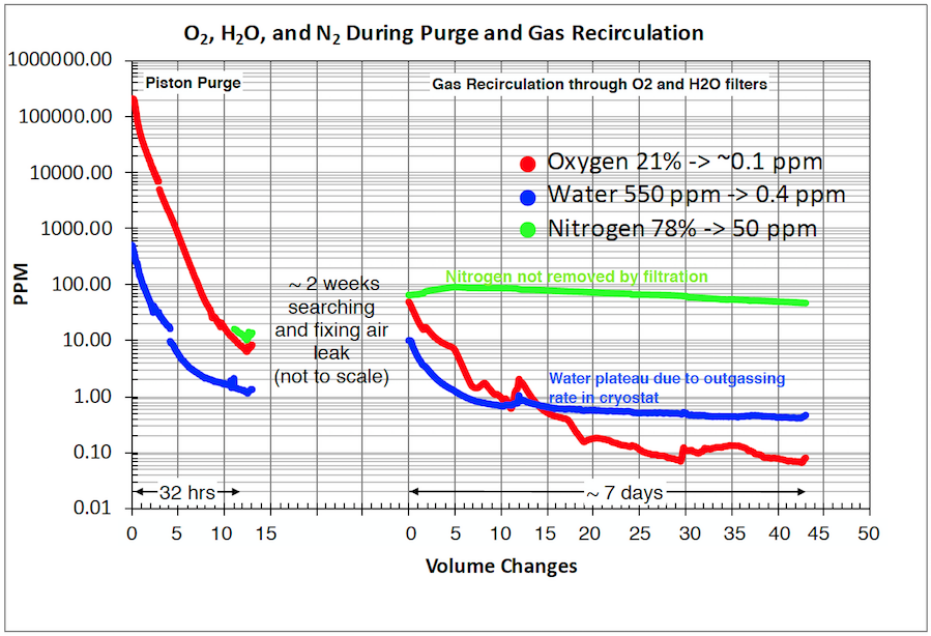

Figure 1.24: Plot of the O_2, H_2O, and N_2 levels during the piston purge and gas recirculation stages of the 35 ton prototype Phase 1 run

Since any one gas analyzer covers only one contaminant species and a range of 3 to 4 orders of magnitude, several units are needed both for the three contaminant gases and to cover the ranges seen between cryostat closure and the beginning of TPC operations: 20 % to $\lesssim$ 100 ppt for O_2, 80 % to $\lesssim$ 1 ppm for N_2, and $\sim$ 1 % to $\lesssim$ 1 ppb for H_2O. Because the total cost of these analyzers exceeds \$100 k, we want to be able to sample more than a single location or cryostat with the same gas analyzers. At the same time, the tubing run lengths from the sample point should be as short as possible to maintain a timely response for the gas analyzer. This puts some constraints on sharing devices because, for example, a separate gas analyzer may be required in the storage infrastructure for argon delivery at the surface.

1.2.6 Cameras

Cameras provide direct visual information about the state of the detector module during critical operations and when damage or unusual conditions are suspected. Cameras in the WA105 DP demonstrator showed spray from cooldown nozzles and the level and state of the LAr as it covered the charge-readout plane (CRP) [9]. A camera was used in the Liquid Argon Purity Demonstrator cryostat[8] to study HV discharges in LAr and in EXO-100 while a TPC was operating [10]. Warm

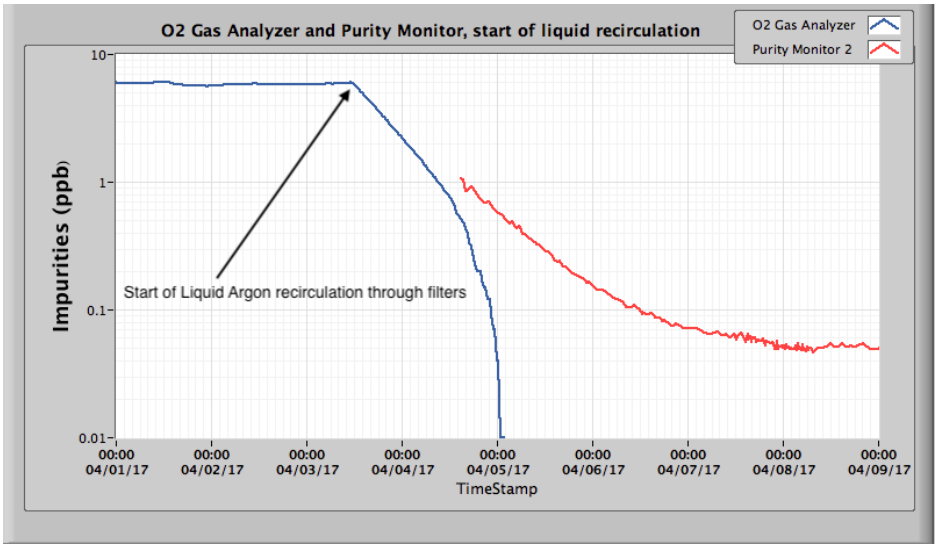

Figure 1.25: O_2 as measured by a precision O_2 analyzer just after the 35 ton prototype cryostat was filled with LAr, continuing with the LAr pump start and beginning of LAr recirculation through the filtration system. As the gas analyzer loses sensitivity, the purity monitor can pick up the impurity measurement. Note that the purity monitor is sensitive to both O_2 and H_2O impurities giving rise to its higher levels of impurity.

cameras viewing LAr from a distance have been used to observe HV discharges in LAr in fine detail [11]. Cameras are commonly used during calibration source deployment in many experiments (e.g., the KamLAND ultra-clean system [12]).

In DUNE, cameras will verify the stability, straightness, and alignment of the hanging TPC structures during cooldown and filling; to ensure that no bubbling occurs near the GPs (SP) or CRPs (DP); to inspect the state of movable parts in the detector module (calibration devices, dynamic thermometers); and to closely inspect parts of the TPC after any seismic activity or other unanticipated event. For these functions, a set of fixed *cold* cameras are used; they are permanently mounted at fixed points in the cryostat for use during filling and commissioning, and a movable, replaceable *warm* inspection camera can be deployed through any free instrumentation flange at any time during the life of the experiment.

Eleven cameras were deployed in ProtoDUNE-SP at the locations shown in Figure 1.26. They successfully provided views of the detector during filling and throughout its operation.

The following sections describe the design considerations for both cold and warm cameras and the associated lighting system. ProtoDUNE-SP camera system designs and performance are also discussed. The same basic designs can be used for both the SP and DP detector modules.

1.2.6.1 Cryogenic Cameras (Cold)

The fixed cameras monitor the following items during filling:

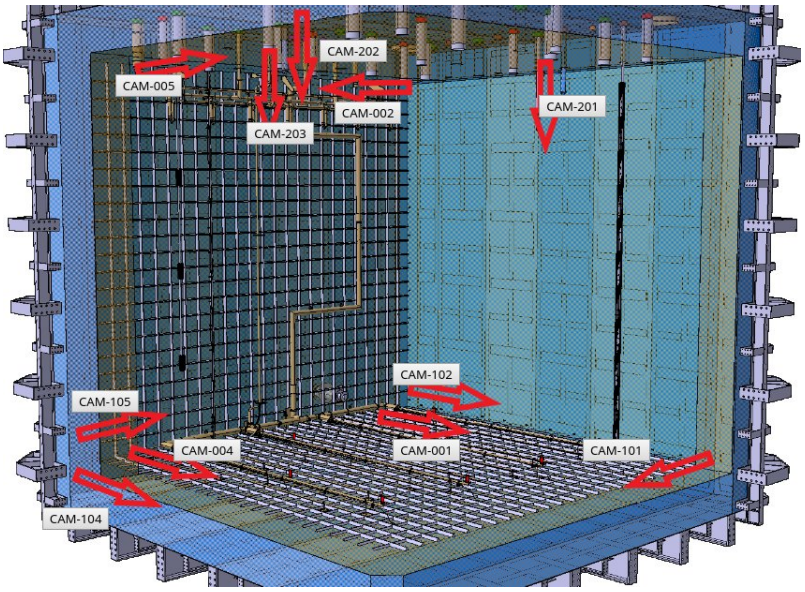

Figure 1.26: A 3D view showing the locations of the 11 cameras in ProtoDUNE-SP.

- positions of corners of APA or CRP, cathode plane assembly (CPA) or cathode, FCs, GPs (1 mm resolution)
- relative straightness and alignment of APA or CRP, CPA or cathode, and FC ($\lesssim 1$ mm)
- relative positions of profiles and endcaps (0.5 mm resolution); and
- the LAr surface, specifically, the presence of bubbling or debris.

One design for the DUNE fixed cameras uses an enclosure similar to the successful EXO-100 design [10], which was also successfully used in the Liquid Argon Purity Demonstrator and ProtoDUNE-SP (see Figure 1.27). Cameras 101, 102, 104, and 105, shown in Figure 1.26, use this enclosure. A thermocouple in the enclosure allows temperature monitoring, and a heating element provides temperature control. SUB-D connectors are used at the cryostat flanges and the camera enclosure for signal, power, and control connections.

An alternative design uses an acrylic enclosure. This design was used successfully in ProtoDUNE-SP (see Figure 1.27, bottom left). Cameras 001, 002, 004, and 005, shown in Figure 1.26, use acrylic enclosures. All operate successfully, including those at the bottom of the cryostat. It must be noted that the DUNE FD will be twice as deep as ProtoDUNE, and therefore cameras observing the lowest surfaces of the FC must withstand twice the pressure.

Improved designs for the cold cameras will be tested in ProtoDUNE-DP and CITF for improved imaging including focus adjustment, and in CITF for pressure resistance, during 2020.

1.2.6.2 Inspection Cameras (Warm)

The inspection cameras are intended to be as versatile as possible. However, the following inspections have been identified as likely uses:

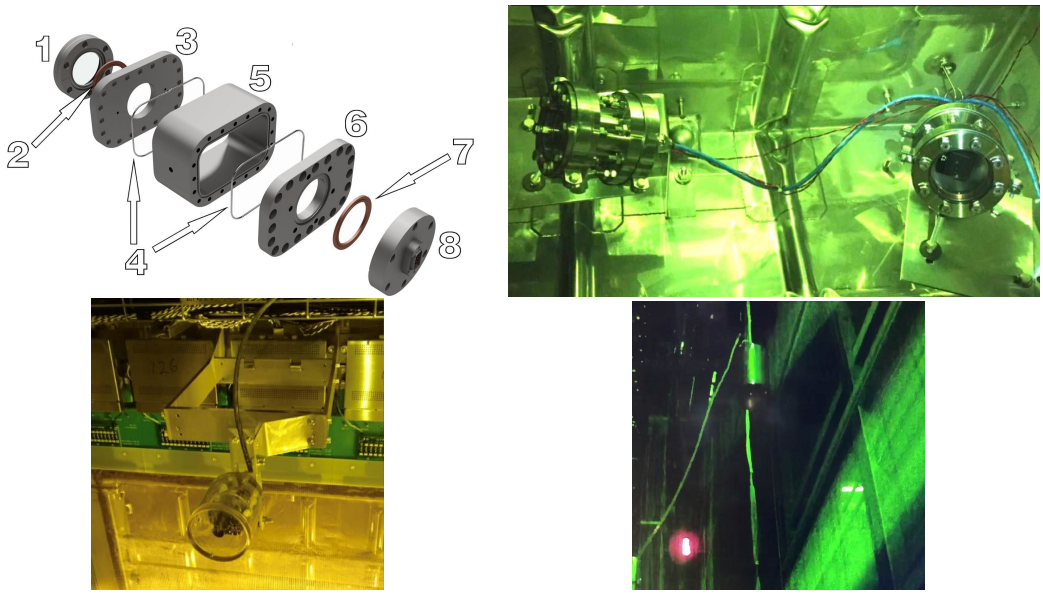

Figure 1.27: Top left: a CAD exploded view of a vacuum-tight camera enclosure suitable for cryogenic applications [10]. (1) quartz window, (2 and 7) copper gasket, (3 and 6) flanges, (4) indium wires, (5) body piece, (8) signal feedthrough. Top right: two of the ProtoDUNE-SP cameras using a stainless steel enclosure. Bottom left: one of the ProtoDUNE-SP cameras using acrylic enclosure. Bottom right: a portion of an image taken with ProtoDUNE-SP camera 105 showing a purity monitor mounted outside the APA on the beam left side. This photo was taken with ProtoDUNE-SP completely filled.

- status of HV feedthrough and cup,
- status of FC profiles, endcaps (0.5 mm resolution),
- vertical deployment of calibration sources,
- status of thermometers, especially dynamic thermometers,
- HV discharge, corona, or streamers on HV feedthrough, cup, or FC,
- relative straightness and alignment of APA/CRP, CPA/cathode, and FC (1 mm resolution),
- gaps between CPA frames (1 mm resolution),
- relative position of profiles and endcaps (0.5 mm resolution), and
- sense wires at the top of outer wire planes in SP APA (0.5 mm resolution).

Unlike the fixed cameras, the inspection cameras must operate only as long as inspection lasts; the cameras can be replaced in case of failure. It is also more practical to keep the cameras continuously warmer than −150 °C during deployment; this allows use of commercial cameras, e.g., cameras of the same model were used successfully to observe discharges in LAr from 120 cm away [11].

The inspection cameras use the same basic enclosure design as for cold cameras, but the cameras are mounted on a movable fork so that each camera can be inserted and removed from the cryostat, using a design similar to the dynamic temperature probes: see Figure 1.28 (left) and Figure 1.9. To avoid contaminating the LAr with air, the entire system is sealed, and the camera can only be deployed through a feedthrough equipped with a gate valve and a purging system, similar to the one used in the vertical axis calibration system at KamLAND [12]. The entire system is purged with pure argon gas before the gate valve is opened.

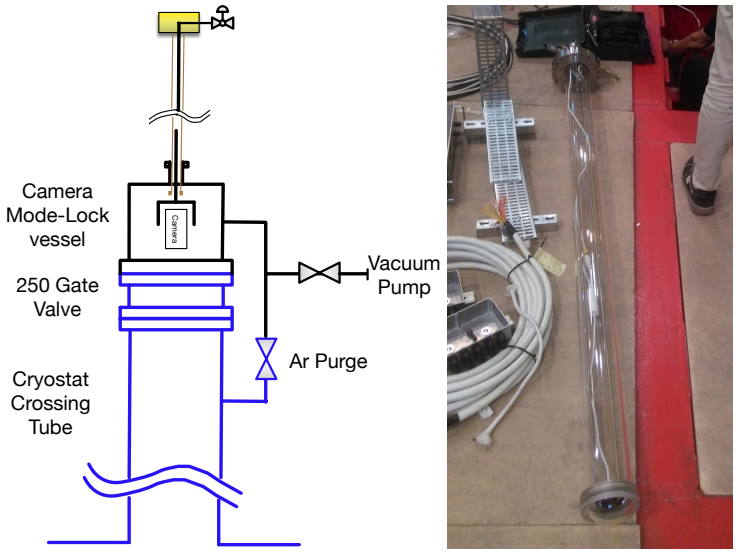

Figure 1.28: Left: An overview of the inspection camera design using a sealed deployment system opening directly into the cryostat. Right: A photo of the ProtoDUNE-SP warm inspection camera acrylic tube, immediately before installation; the acrylic tube is sealed with an acrylic dome at the bottom and can be opened at the top.

Motors above the flange allow the fork to be rotated and moved vertically to position the camera. A chain drive system with a motor mounted on the end of the fork allows the camera assembly to tilt, creating a point-tilt mount that can be moved vertically. With the space above the cryostat flanges and the thickness of the cryostat insulation, cameras can be moved vertically up to 1 m inside the cryostat.

The motors for rotation and vertical motion are outside the sealed volume, coupled mechanically using ferrofluidic seals, thus reducing any risk of contamination and allowing manual rotation of the vertical drive in the event of motor failure.

An alternative design was demonstrated in ProtoDUNE-SP. In this design, the warm camera is contained inside a gas-tight acrylic tube inserted into the feedthrough, so a gate valve or a gas-tight rotatable stage is not needed, and the warm cameras can be removed for servicing or upgrade at any time. Figure 1.28 (right) shows an acrylic tube enclosure and camera immediately before deployment. These acrylic tube enclosures for removable cameras were deployed at the positions marked 201, 202, and 203 in Figure 1.26; they operated successfully in ProtoDUNE-SP. Cameras with fisheye lenses were used in these tubes during initial operation. One camera was removed without any evidence of contamination of the LAr. We plan to use other cameras during post-beam running.

Improved designs for the inspection cameras will be tested in the CITF and ProtoDUNE-SP during 2020 and 2021, focusing particularly on longevity, camera replaceability, and protection of the LAr.

1.2.6.3 Light-emitting system

The light-emitting system uses LEDs to illuminate the parts of the detector module in the camera's field of view with selected wavelengths (IR and visible) that cameras can detect. Performance criteria for the light-emission system include the efficiency with which the cameras can detect the light and the need to avoid adding heat to the cryostat. Very high-efficiency LEDs help reduce heat generation; one 750 nm LED [13] has a specification equivalent to 33 % conversion of electrical input power to light.

While data on how well LEDs perform at cryogenic temperatures is sparse, some studies of NASA projects [14] indicate that LED are more efficient at low temperatures and that emitted wavelengths may change, particularly for blue LEDs. In ProtoDUNE-SP, amber LEDs were observed to emit green light at LAr temperature (see bottom right photo in 1.27). To avoid degradation of wavelength-shifting materials in the PD system, short wavelength LEDs are not used in the FD; LEDs will be tested in LN to ensure their wavelength is long enough.

LEDs are placed in a ring around the outside of each camera, pointing in the same direction as the lens, to illuminate nearby parts of the detector module within the camera's field of view. Commercially available LEDs exist with a range of angular spreads that can be matched to the needs of the cameras without additional optics.

Additionally, chains of LEDs connected in series and driven with a constant-current circuit are used for broad illumination, with each LED paired in parallel with an opposite polarity LED and a resistor (see Figure 1.29). This allows two different wavelengths of illumination using a single chain simply by changing the direction of the drive current, and allows continued use of an LED chain even if individual LEDs fail.

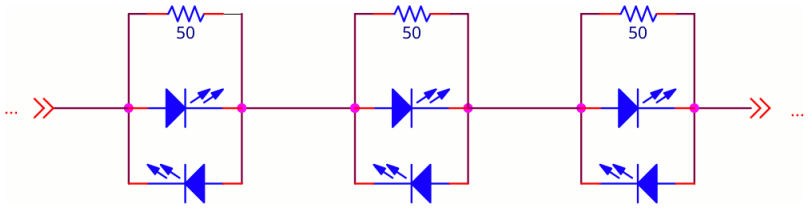

Figure 1.29: Example schematic for LED chain, allowing failure tolerance and two LED illumination spectra.

1.2.7 Cryogenic Instrumentation Test Facility

The CISC consortium plans to build a cryogenic instrumentation test facility (CITF) at Fermilab to facilitate testing of various cryogenic instrumentation devices and small-scale assemblies of CISC systems. In the past and recent times, various test facilities at Fermilab have provided access to small ($<$ 1 ton) to intermediate ($\sim$ 1 ton) volumes of purified TPC-grade LAr, required for any device intended for drifting electrons for millisecond periods.

The Proton Assembly Building (PAB) facility at Fermilab houses the ICEBERG 3000 liter cryostat

which enables fast turnaround testing for the DUNE cold electronics (CE).

The PAB facility also includes TallBo (450 liter), Blanche (500 liter), and Luke (250 liter) cryostats. In the recent past, Blanche has been used for HV studies, TallBo for PD studies, and Luke for the material test stand work. These studies have contributed to the design and testing of ProtoDUNE-SP components.

1.2.8 Validation in ProtoDUNE

Design validation and testing of many planned CISC systems for the SP module will be done using the data from ProtoDUNE-SP and ProtoDUNE-DP as discussed below.

- **Level Meters:** The same differential pressure level meters which are already validated in ProtoDUNE-SP will be used in SP module. The same capacitive level meters currently used in ProtoDUNE-DP will be used in the SP module. These will be validated in the upcoming ProtoDUNE-DP run.
- **Pressure Meters (GAr):** Same high precision pressure sensors which are already validated in ProtoDUNE-SP will be used in SP FD.
- **Gas Analyzers:** The same gas analyzers currently used in ProtoDUNE-SP will be used in the SP module so they have already been validated.
- **High precision thermometer arrays in LAr:** The static and dynamic T-gradient thermometers discussed in the previous sections are validated using ProtoDUNE-SP data.
- **Purity monitors:** The same purity monitor basic design used in ProtoDUNE-SP will be used in the FD SP module. ProtoDUNE-SP and ProtoDUNE-DP run 2 phase provides opportunities to test any improvements to the design.
- **Cameras:** various types of cameras are being actively developed in both ProtoDUNE-SP and ProtoDUNE-DP so the validation of designs will be performed both at ProtoDUNE-SP and ProtoDUNE-DP. Future improvements can be tested in ProtoDUNE-SP and ProtoDUNE-DP run 2 phase at CERN.

1.3 Slow Controls

The slow controls system collects, archives, and displays data from a broad variety of sources and provides real-time status, alarms, and warnings for detector operators. The slow control system also provides control for items such as HV systems, TPC electronics, and PD systems. Data is acquired via network interfaces. Figure 1.30 shows connections between major parts of the slow controls system and other systems.

The ProtoDUNE-SP detector control system[5] fully met its operational requirements. Section 1.3.6 provides a short description of the ProtoDUNE-SP slow controls and its performance.

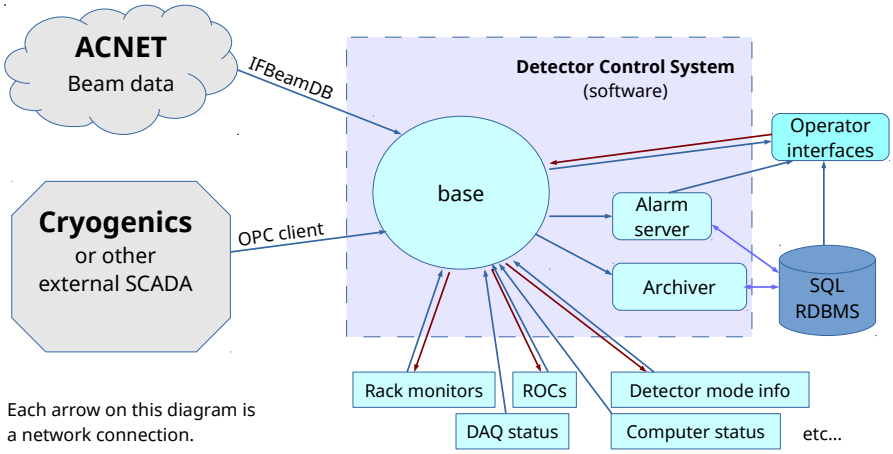

Figure 1.30: Typical slow controls system connections and data flow

1.3.1 Slow Controls Hardware

Slow controls is expected to need a modest amount of dedicated hardware, largely for rack monitoring, and a small amount of dedicated network and computing hardware. Slow controls also relies on common infrastructure as described in Section 1.3.2.

1.3.1.1 Dedicated Monitoring Hardware

Every rack (including those in the central utility cavern (CUC)) should have dedicated hardware to monitor rack parameters like rack protection system, rack fans, rack air temperatures, thermal interlocks with power supplies, and any interlock bit status monitoring needed for the racks. For the racks in the CUC server room, this functionality is built into the proposed water cooled racks, as already in place at ProtoDUNE. For the racks on the detector itself, the current plan is to design and install a custom-built 1U rack-mount enclosure containing a single-board computer to control and monitor various rack parameters. Such a system has been successfully used in MicroBooNE. The design is being improved for the short-baseline near detector (SBND) experiment (see Figure 1.31). Other slow controls hardware includes interfacing cables like adapters for communication and debugging and other specialized cables like GPIB or National Instruments cables. The cable requirements must be determined in consultation with other groups once hardware choices for various systems are finalized.

1.3.1.2 Slow Controls Network Hardware

The slow controls data originates from the cryogenic instrumentation and from other systems as listed in Table 1.5. This data is collected by software running on servers (Section 1.3.1.3) housed in the underground data room in the CUC, where data is archived in a central CISC database. The instrumentation data is transported over conventional network hardware from any sensors located

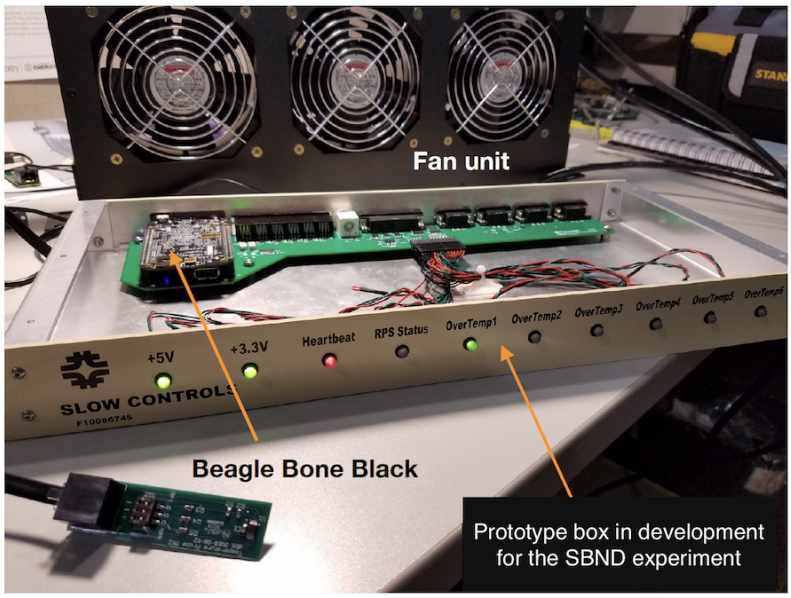

Figure 1.31: Rack monitoring box prototype in development for the short-baseline near detector (SBND) experiment based on the original design from MicroBooNE.

in the cryogenic plant. However, the readouts that are in the racks on top of the cryostats must be cautious about grounding and noise. Therefore, each rack on the cryostat has a small network switch that sends any network traffic from that rack to the CUC via a fiber transponder. This is the only network hardware specific to slow controls and will be provided by SURF's general computing infrastructure. The network infrastructure requirements are described in Section 1.3.2.

1.3.1.3 Slow Controls Computing Hardware

Two servers (a primary server and a replicated backup) suitable for the relational database discussed in Section 1.3.3 are located in the CUC data room, with an additional two servers to service the FE monitoring interface; such service would include assembling dynamic CISC monitoring web pages from adjacent databases. Another server will be needed to run back-end I/O. Any special purpose software, such as iFix used by the cryogenics experts, would also run here. One or two additional servers should accommodate these programs. Replicating this setup on a per-module basis would make commissioning and independent operation easier, accommodate different module design (and the resulting differences in database tables), and ensure sufficient capacity. These four sets of networking hardware would fit tightly into one rack or very comfortably into two. Using the requirements from CISC, the DAQ consortium will provide the needed cost for servers and racks.

1.3.2 Slow Controls Infrastructure

The data rate will be in the range of tens of kilobytes per second, given the total number of slow controls quantities and the update rate (see Section 1.3.4), placing minimal demands on local

network infrastructure. Network traffic out of SURF to Fermilab will primarily be database calls to the central CISC database, either from monitoring applications or from database replication to the offline version of the CISC database. This traffic requires little bandwidth, so the proposed general purpose links both out of the underground area at SURF and back to Fermilab can accommodate the traffic.

Up to two racks of space and appropriate power and cooling are available in the CUC's DAQ server room for CISC use. This is ample space as described in Section 1.3.1.3.

1.3.3 Slow Controls Software

To provide complete monitoring and control of detector subsystems, the slow controls software includes

- the control systems base for input and output operations and defining processing logic, scan conditions, and alarm conditions;
- an alarm server to monitor all channels and send alarm messages to operators;
- a data archiver for automatic sampling and storing values for history tracking; and
- an integrated operator interface providing display panels for controls and monitoring.

In addition, the software must be able to interface indirectly with external systems (e.g., cryogenics control system) and databases (e.g., beam database) to export data into slow controls process variables (or channels) for archiving and status displays. This allows us to integrate displays and warnings into one system for the experiment operators and provides integrated archiving for sampled data in the archived database. As one possibility, an input output controller running on a central DAQ server could provide soft channels for these data. Figure 1.30 shows a typical workflow of a slow controls system.

The key features of the software require highly evolved software designed to manage real-time data exchange, scalable to hundreds of thousands of channels sampled at intervals of hours to seconds as needed. The software must be well documented, supported, and reliable. The base software must also allow easy access to any channel by name. The archiver software must allow data storage in a database with adjustable rates and thresholds so data for any channel can be easily retrieved using channel name and time range. Among other key features, the alarm server software must remember the state, support an arbitrary number of clients, and provide logic for delayed alarms and acknowledging alarms. A standard naming convention for channels will be part of the software to help handle large numbers of channels and subsystems.

The ProtoDUNE-SP detector control system software [5] provides a prototype for the FD slow controls software. In ProtoDUNE-SP, the unified control system base is WinCC OA [15], a commercial toolkit used extensively at CERN, with device interfaces supported using several standardized interface protocols. A more detailed description is in Section 1.3.6 below. WinCC OA is our baseline for the FD slow control software. EPICS [16] is an alternative controls system which also meets the specifications; it is used in other neutrino experiments including MicroBooNE [17] and NOvA [18].

1.3.4 Slow Controls Quantities

The final set of quantities to monitor will ultimately be determined by the subsystems being monitored, documented in appropriate interface control documents (ICDs), and continually revised based on operational experience. The total number of quantities to monitor has been roughly estimated by taking the total number monitored in ProtoDUNE-SP[5], 7595 as of Nov. 19, 2018, and scaling by the detector length and the number of planes, giving approximately 150,000 per detector module. Quantities should update on average no more than once per minute. Transmitting a single update for each channel at that rate translates to a few thousand updates per second, or a few tens of thousands of bytes per second. While this is not a significant load on a network with an efficient slow controls protocol, it would correspond to approximately 1 TB per year per detector module if every timestamp and value were stored. The actual data volume will be less because values are stored only if they vary from previous values by more than an amount that is adjustable channel-by-channel. Database storage also allows data to be sparsified later. No slow controls data is planned to be written to the DAQ stream. With careful management of archiving thresholds for each quantity monitored and yearly reduction of stored sample time density, the retained data volume can be reduced to a few TB over the life of the experiment.

The subsystems to be monitored include the cryogenic instrumentation described in this chapter, the other detector systems, and relevant infrastructure and external devices. Table 1.5 lists the quantities expected from each system.

1.3.5 Local Integration

The local integration of the slow controls consists entirely of software and network interfaces with systems outside of the scope of the detector module. This includes the following:

- readings from the LBNF-managed external cryogenics systems, for status of pumps, flow rates, inlet, and return temperature and pressure, which are implemented via OPC or a similar SCADA interface;
- beam status, such as protons-on-target, rate, target steering, and beam pulse timing, which are retrieved via IFbeam; and
- near detector status, which can be retrieved from a common slow controls database.

Integration occurs after both the slow controls and non-detector systems are in place. The LBNF-CISC interface is managed by the cryogenics systems working group in CISC as described in Section 1.4, which includes members from both CISC and LBNF. The IFbeam interface for slow controls is already well established in MicroBooNE, NOvA, and other Fermilab experiments. An internal near-detector–FD working group can be established to coordinate detector status exchange between the near and far sites.

Table 1.5: Slow controls quantities

System	Quantities
Detector cryogenic instrumentation	
Purity monitors	anode and cathode charge, bias voltage and current, flash lamp status, calculated electron lifetime
Thermometers	temperature, position of dynamic thermometers
Liquid level	liquid level
Gas analyzers	purity level readings
Pressure meters	pressure readings
Cameras	camera voltage and current draw, temperature, heater current and voltage, lighting current and voltage
Other detector systems	
Cryogenic internal piping	feedthrough gas purge flow and temperature
HV systems	drift HV voltage and current, end-of-field cage current and bias voltage, electron diverter bias, ground plane currents
TPC electronics	voltage and current to electronics
PD	voltage and current for photodetectors and electronics
DAQ	warm electronics currents and voltages, run status, DAQ buffer sizes, trigger rates, data rates, GPS status, computer and disk health status, other health metrics as defined by DAQ group
CRP / APA	bias voltages and currents
Infrastructure and external systems	
Cryogenics (external)	status of pumps, flow rates, inlet and return temperature and pressure (via OPC or similar SCADA interface)
Beam status	protons on target, rate, target steering, beam pulse timing (via IFbeam)
Near detector	near detector run status (through common slow controls database)
Rack power and status	power distribution unit current and voltage, air temperature, fan status if applicable, interlock status
Detector calibration systems	
Laser	laser power, temperature, operation modes, other system status as defined by calibration group
External neutron source	safety interlock status, power supply monitoring, other system status as defined by calibration group
External radioactive source	system status as defined by calibration group

1.3.6 Validation in ProtoDUNE

The ProtoDUNE-SP detector control system has met all requirements for operation of ProtoDUNE-SP [5] and will be used for ProtoDUNE-DP. The requirements for ProtoDUNE are nearly identical to those for the SP module other than total channel count. Of particular note, the ProtoDUNE slow control system unified a heterogenous set of devices and data sources through several protocols into a single control system, as illustrated in Figure 1.32. In addition to what the figure shows, data were also acquired from external cryogenic and beam systems. The topology and data flow of the system matches the general shape shown in Figure 1.30.

In this control system, the unified control system base is WinCC-OA [15], a commercial SCADA system for visualizing and operating of processes, production flows, machines, and plants, used in many businesses. It was chosen at European Organization for Nuclear Research (CERN) as a basis for developing the control systems of the LHC experiments, the accelerators and the laboratory infrastructure for its flexibility and scalability, as well as for the openness of the architecture, allowing it to interface with many different types of hardware devices and communication protocols. Additional software developed at CERN is also used, including Joint COntrols Projects [19] and UNified Industrial COntrol System (UNICOS) [20]. WinCC-OA and the additional software developed on top of it in the past 20 years, have grown into a fairly complex ecosystem. While multiple collaboration members have experience using the ProtoDUNE-SP control system, customising and using WinCC-OA in an effective way for developing the control system of DUNE requires proper training and a non-negligible learning effort.

As noted in Sections 1.3.3 and 1.3.4, the slow control archiver will gradually accumulate terabytes of data, requiring a sizable database to store the value history and allow efficient data retrieval. Individually adjustable rates and thresholds for each channel are key to keeping this database manageable. The ProtoDUNE-SP operations provided not only a test of these features as implemented in the ProtoDUNE slow control system, but also insight into reasonable values for these archiving parameters for each system.

1.4 Organization and Management

The organization of the CISC consortium is shown in Figure 1.33. The CISC consortium board currently comprises institutional representatives from 18 institutes as shown in Table 1.6. The consortium leader is the spokesperson for the consortium and responsible for the overall scientific program and managing the group. The technical leader of the consortium is responsible for managing the project for the group. Currently, the consortium has five working groups:

Cryogenics Systems gas analyzers and liquid level monitors; CFD simulations

Argon Instrumentation purity monitors, thermometers, pressure meters, capacitive level meters, cameras and light emitting system, and CITF; feedthroughs; E field simulations; instrumentation precision studies; ProtoDUNE data analysis coordination and validation

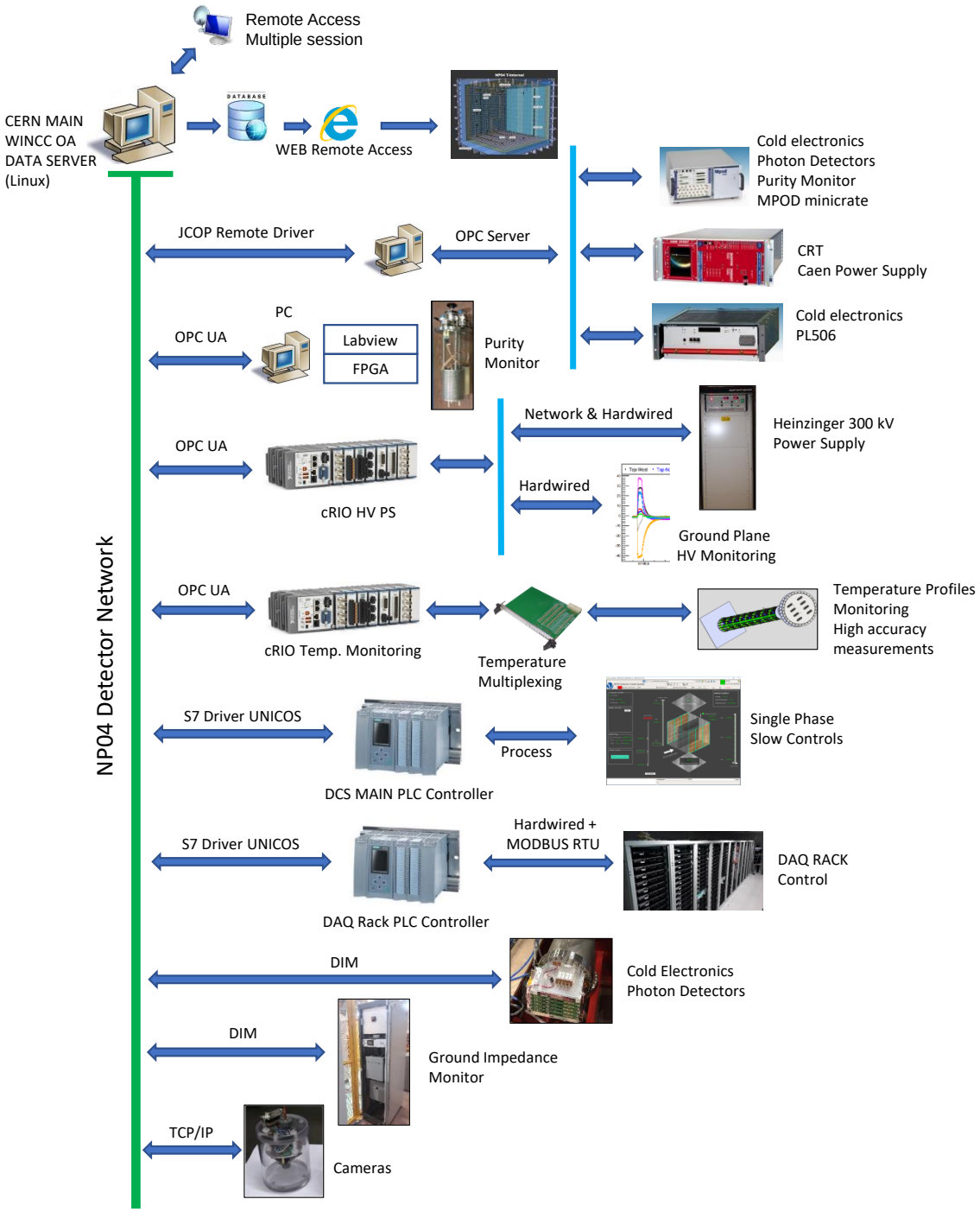

Figure 1.32: Diagram of the ProtoDUNE-SP control system topology, from [5].

Slow Controls Base Software and Databases base I/O software, alarms and archiving databases, and monitoring tools; variable naming conventions and slow controls quantities

Slow Controls Detector System Interfaces signal processing software and hardware interfaces (e.g., power supplies); firmware; rack hardware and infrastructure

Slow Controls External Interfaces interfaces with external detector systems (e.g., cryogenics system, beam, facilities, DAQ, near detector status)

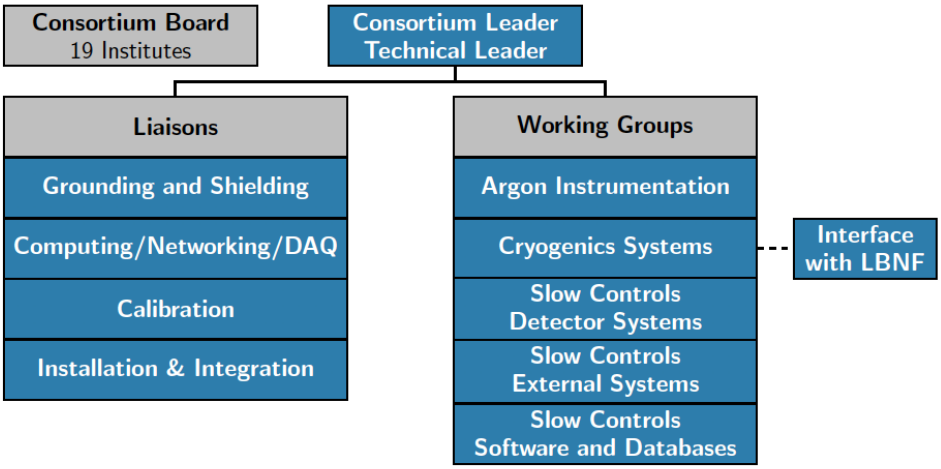

Figure 1.33: CISC Consortium organizational chart

Moreover, because the CISC consortium broadly interacts with other groups, liaisons have been named as shown in Figure 1.33. A short-term task force was recently formed to explore the need for cryogenic modeling for the consortium. A work plan for CFD simulations for both ProtoDUNE and FD was developed based on input from the task force.

1.4.1 Institutional Responsibilities

The CISC consortium will be a joint effort for SP and DP. A single slow controls system will be implemented to serve both the SP module and the DP module.

Design and installation of cryogenic systems (e.g., gas analyzers, liquid level monitoring) will be coordinated with LBNF, with the consortium providing resources and effort, and expertise provided by LBNF. ProtoDUNE designs for LAr instrumentation (e.g., purity monitors, thermometers, cameras) will be the basis for detector module designs. Design validation, testing, calibration, and performance will be evaluated through ProtoDUNE data.

Following the conceptual funding model envisioned for the consortium, various responsibilities have been distributed across institutions within the consortium. At this stage of the project, firm funding decisions are not made yet. Table 1.7 shows the current institutional responsibilities for

Table 1.6: Current CISC consortium board members and their institutional affiliations

Member Institute	Country
CIEMAT	Spain
Instituto de Fisica Corpuscular (IFIC)	Spain
University of Warwick	UK
University College London (UCL)	UK
Argonne National Lab (ANL)	USA
Brookhaven National Lab (BNL)	USA
University of California, Irvine (UCI)	USA
Drexel University	USA
Fermi National Accelerator Lab (Fermilab)	USA
University of Hawaii	USA
University of Houston	USA
Idaho State University (ISU)	USA
Kansas State University (KSU)	USA
University of Minnesota, Duluth (UMD)	USA
Notre Dame University	USA
South Dakota State University (SDSU)	USA
University of Tennessee at Knoxville (UTK)	USA
Virginia Tech (VT)	USA
Boston University (BU)	USA

primary CISC subsystems. Only lead institutes are listed in the table for a given effort. For physics and simulations studies, and validation efforts with ProtoDUNE, a number of institutes are involved. A detailed list of tasks and institutional responsibilities are presented in [21].

Table 1.7: Institutional responsibilities in the CISC consortium

CISC Sub-system	Institutional Responsibility
Purity Monitors	UCI, Houston
Static T-gradient monitors	IFIC
Dynamic T-gradient monitors	Hawaii
Individual Sensors	IFIC
Readout System for Thermometers	IFIC, Hawaii, CIEMAT
Pressure Meters	UTK
Cold Cameras	KSU, BNL
Warm Cameras	KSU, BNL
Light-emitting System (for cameras)	Drexel
Gas Analyzers	FNAL, LBNF
Differential Pressure Level Meters	LBNF
Capacitive Level Meters	Notre Dame
cryogenic instrumentation test facility (CITF)	FNAL, ANL
CFD Simulations	SDSU, ANL
Other Simulation & Validation Studies	Number of Institutes
Slow Controls Hardware	UMD, UTK, Drexel
Slow Controls Infrastructure	UMD, UTK
Slow Controls Base Software	KSU, UTK, BU, Drexel, Warwick, ANL, IFIC
Slow Controls Signal Processing	A number of institutes
Slow Controls External Interfaces	VT, UTK, UMD

1.4.2 Schedule

Table 1.8 shows key construction milestones for the CISC consortium leading to commissioning of the first FD module. CISC construction milestones align with the overall construction milestones of the first FD module (highlighted in orange in the table). The technology design decisions for CISC systems should be made by April 2020 followed by final design reviews in June 2020. Design decisions will largely be based on how a given system performed (technically and physics-wise) in ProtoDUNE. This is currently actively ongoing with the ProtoDUNE-SP instrumentation data. As noted in Section 1.2.8, the current plan is to deploy improved designs of static and dynamic T-gradient thermometers, purity monitors, long (DP-style) level meters and cameras to be validated in ProtoDUNE-2. The production of systems aimed for ProtoDUNE-2 SP should be finished by January 2021 followed by assembly and deployment in March 2021.

Designs may need review based on performance in ProtoDUNE-2 and any modifications will be

Table 1.8: CISC construction schedule milestones leading to commissioning of the first FD module. Key DUNE dates and milestones, defined for planning purposes in this TDR, are shown in orange. Dates will be finalized following establishment of the international project baseline.

Milestone	Date (Month YYYY)
Technology Decision Dates	April 2020
Final Design Review Dates	June 2020
Start of module 0 component production for ProtoDUNE-2	August 2020
End of module 0 component production for ProtoDUNE-2	January 2021
Start of ProtoDUNE-SP-II installation	March 2021
Start of ProtoDUNE-DP-II installation	March 2022
South Dakota Logistics Warehouse available	April 2022
production readiness review (PRR) dates	September 2022
Beneficial occupancy of cavern 1 and CUC	October 2022
Start procurement of CISC hardware	December 2022
CUC counting room accessible	April 2023
Start of production of CISC hardware	April 2023
Top of detector module #1 cryostat accessible	January 2024
End of CISC hardware production	April 2024
Start integration of CISC hardware in the cavern	July 2024
Start of detector module #1 TPC installation	August 2024
Installation of gas analyzers and support structure for all instrumentation devices	September 2024
Installation of individual sensors, static T-gradient thermometers, and level meters	November 2024
Top of detector module #2 cryostat accessible	January 2025
All slow controls hardware, infrastructure, & networking installed	February 2025
Slow controls software for I/O, alarms, archiving, displays installed on production systems	May 2025
End of detector module #1 TPC installation	May 2025
Install dynamic T-gradient monitors, cameras, purity monitors, and pressure meters	June 2025
Install all feedthroughs for instrumentation devices	July 2025
Start of detector module #2 TPC installation	August 2025
Install slow control expert interfaces for all systems in time for testing	September 2025
End of detector module #2 TPC installation	May 2026
Full slow controls systems commissioned and integrated into remote operations	July 2026

incorporated into the final design before the start of production of CISC systems for the FD in April 2023. This will be followed by assembly of the systems underground in the detector cavern in July 2024. Installation of instrumentation devices will start in September 2024 following the beneficial occupancy of the interior of the cryostat. Installing gas analyzers, level meters, individual temperature sensors, static T-gradient thermometers, and support structure for all instrumentation devices will be finished before installing TPC, but installing dynamic T-gradient thermometers, purity monitors, pressure meters and cameras will occur afterward. CISC will work closely with LBNF to coordinate installation of the cryogenic systems and instrumentation devices. For slow controls, the goal is to have the full slow controls system commissioned and integrated into remote operations at least three months before the SP module is ready for operations.

1.4.3 Risks

Table 1.9 lists the possible risks identified by the CISC consortium along with corresponding mitigation strategies. A more detailed list of risks with additional descriptions can be found in [22]. The table shows 18 risks, all at medium or low level, mitigated with necessary steps and precautions. More discussion on all medium-level risks are provided in the text below.

- Risk 01: The risk associated with ProtoDUNE-SP-based designs being inadequate for FD, is important because this requires early validation from ProtoDUNE data so R&D of alternate designs can be timely. With ProtoDUNE-SP data now available, the consortium is focused on validating instrumentation designs.
- Risk 06: Temperature sensors in the dynamic T-gradient monitor are calibrated using two methods: lab calibration to 0.002 K (as in the static T-gradient monitor case) and in-situ cross-calibration moving the system vertically. Disagreement between the two methods can occur. In order to mitigate this we need to investigate and improve both methods, specifically the laboratory calibration since this is the only one possible for sensors behind APAs, and top/bottom of the detector.
- Risk 10: This risk involves not being able to build a working prototype for cold cameras during R&D phase that meets all the requirements & safety. For example, cold camera prototypes fail longevity tests or show low performance (e.g. bad resolution). This risk originates from past experience with cold cameras that became non-operational after a period of time in LAr or show low performance. In order to address this, we plan to pursue further R&D to improve thermal insulation and heaters, develop alternative camera models, etc. If problems persist one can use the cameras in the ullage (cold or inspection) with the appropriate field of view and lighting such that elements inside LAr can be inspected during filling.
- Risk 12: Cameras are delicate devices and some of them located near HV devices can be destroyed by HV discharges. This can be mitigated by ensuring that most important cold cameras have enough redundancy such that the loss of one camera does not compromise the overall performance. In the case of inspection cameras since they are replaceable, one can simply replace them.
- Risk 17: The gas analyzers and level meters may fail as these are commercial devices purchased at some point in their product cycle and cannot be required to last 20 years. Typical

warranties are ∼1 year from date of purchase. The active electronics parts of both gas analyzers and level meters are external to the cryostat so they can be replaced. To mitigate this, provisions will be made for future replacement in case of failure or loss of sensitivity. Also, the risk is not high since we have purity monitors in the filtration system that can cover the experiment during the time gas analyzers are being replaced or repaired.

Related to risks 12, 16 and 18, aging is an important aspect for several monitors, especially for those that are inaccessible. The ProtoDUNE tests demonstrate that the devices survive the commissioning phase and we continue to learn from ProtoDUNE experience. In addition to ProtoDUNE, other tests are planned. For example, in the case of purity monitors, photocathodes are expected to survive the first five years and if we prevent running them with high frequency at low purity (lifetime < 3 ms), aging can be prevented for a longer time. To understand long-term aging, R&D is planned at CITF and at member institute sites for many of the devices. Other systems that are replaceable such as inline purity monitors, gas analyzers, and inspection cameras can be replaced when failures occur and maintained for the lifetime of the experiment.

Table 1.9: Risks for SP-FD-CISC (P=probability, C=cost, S=schedule) More information at risk probabilities. ref `tab:risks:SP-FD-CISC`

ID	Risk	Mitigation	P	C	S
RT-SP-CISC-01	Baseline design from ProtoDUNEs for an instrumentation device is not adequate for DUNE far detectors	Focus on early problem discovery in ProtoDUNE so any needed redesigns can start as soon as possible.	L	M	L
RT-SP-CISC-02	Swinging of long instrumentation devices (T-gradient monitors or PrM system)	Add additional intermediate constraints to prevent swinging.	L	L	L
RT-SP-CISC-03	High E-fields near instrumentation devices cause dielectric breakdowns in LAr	CISC systems placed as far from cathode and FC as possible.	L	L	L
RT-SP-CISC-04	Light pollution from purity monitors and camera light emitting system	Use PrM lamp and camera lights outside PDS trigger window; cover PrM cathode to reduce light leakage.	L	L	L
RT-SP-CISC-05	Temperature sensors can induce noise in cold electronics	Check for noise before filling and remediate, repeat after filling. Filter or ground noisy sensors.	L	L	L
RT-SP-CISC-06	Disagreement between lab and *in situ calibrations for ProtoDUNE-SP dynamic T-gradient monitor*	Investigate and improve both methods, particularly laboratory calibration.	M	L	L
RT-SP-CISC-07	Purity monitor electronics induce noise in TPC and PDS electronics.	Operate lamp outside TPC+PDS trigger window. Surround and ground light source with Faraday cage.	L	L	L

RT-SP-CISC-08	Discrepancies between measured temperature map and CFD simulations in ProtoDUNE-SP	Improve simulations with additional measurements inputs; use fraction of sensors to predict others	L	L	L
RT-SP-CISC-09	Difficulty correlating purity and temperature in ProtoDUNE-SP impairs understanding cryo system.	Identify causes of discrepancy, modify design. Calibrate PrM differences, correlate with RTDs.	L	L	L
RT-SP-CISC-10	Cold camera R&D fails to produce prototype meeting specifications & safety requirements	Improve insulation and heaters. Use cameras in ullage or inspection cameras instead.	M	M	L
RT-SP-CISC-11	HV discharge caused by inspection cameras	Study E-field in and on housing and anchoring system. Test in HV facility.	L	L	L
RT-SP-CISC-12	HV discharge destroying the cameras	Ensure sufficient redundancy of cold cameras. Warm cameras are replaceable.	L	M	L
RT-SP-CISC-13	Insufficient light for cameras to acquire useful images	Test cameras with illumination similar to actual detector.	L	L	L
RT-SP-CISC-14	Cameras may induce noise in cold electronics	Continued R&D work with grounding and shielding in realistic conditions.	L	L	L
RT-SP-CISC-15	Light attenuation in long optic fibers for purity monitors	Test the max. length of usable fiber, optimize the depth of bottom PrM, number of fibers.	L	L	L
RT-SP-CISC-16	Longevity of purity monitors	Optimize PrM operation to avoid long running in low purity. Technique to protect/recover cathode.	L	L	L
RT-SP-CISC-17	Longevity: Gas analyzers and level meters may fail.	Plan for future replacement in case of failure or loss of sensitivity.	M	M	L
RT-SP-CISC-18	Problems in interfacing hardware devices (e.g. power supplies) with slow controls	Involve slow control experts in choice of hardware needing control/monitoring.	L	L	L

1.4.4 Interfaces

CISC subsystems interface with all other detector subsystems and potentially impact the work of all detector consortia, as well as some working groups (physics, software/computing, beam instrumentation), and technical coordination, requiring interactions with all of these entities. We also interact heavily with LBNF beam and cryogenics groups. Detailed descriptions of CISC interfaces are maintained in DUNE DocDB. A brief summary is provided in this section. Table 1.10 lists the IDs of the different DocDB documents as well as their highlights. Descriptions of the interfaces and interactions that affect many systems are given below.

CISC interacts with the detector consortia because CISC will provide status monitoring of all important detector sub-systems along with controls for some components of the detector. CISC will also consult on selecting different power supplies to ensure monitoring and control can be established with preferred types of communication. Rack space distribution and interaction between slow controls and other modules from other consortia will be managed by TC in consultation with those consortia.

CISC will work with LBNF to determine whether heaters and RTDs are needed on flanges. If so, CISC will specify the heaters and RTDs, and will provide the readout and control, while the responsibility for the actual hardware will be discussed with the different groups.

Installing instrumentation devices will interfere with other devices and must be coordinated with the appropriate consortia. On the software side, CISC must define, in coordination with other consortia/groups, the quantities to be monitored/controlled by slow controls and the corresponding alarms, archiving, and GUIs.

1.4.5 Installation, Integration, and Commissioning

1.4.5.1 Purity Monitors

The purity monitor system will be built in modules, so it can be assembled outside the cryostat leaving few steps to complete inside the cryostat. The assembly itself comes into the cryostat with the individual purity monitors mounted to support tubes, with no HV cables or optical fibers yet installed. The support tube at the top and bottom of the assembly is then mounted to the brackets inside the cryostat, and the brackets attached to the cables trays and/or the detector support structure. At much the same time, the FE electronics and light source can be installed on the top of the cryostat, and the electronics and power supplies can be installed in the electronics rack.

Integration begins by running the HV cables and optical fibers to the purity monitors, through the top of the cryostat. These cables are attached to the HV feedthroughs with sufficient length to reach each purity monitor inside the cryostat. The cables are run along cable trays through the port reserved for the purity monitor system. Each purity monitor will have three HV cables that connect it to the feedthrough and then further along to the FE electronics. The optical fibers are then run through the special optical fiber feedthrough, into the cryostat, and guided to the purity monitor system either using the cables trays or guide tubes, depending on which solution is adopted. This should protect fibers from breaking accidentally as the rest of the detector and instrumentation installation continues. The optical fibers are then run inside the purity monitor support tube and to the appropriate purity monitor, terminating the fibers at the photocathode of each monitor while protecting them from breaking near the purity monitor system itself.

Integration continues as the HV cables are connected through the feedthrough to the system FE electronics; then optical fibers are connected to the light source. The cables connecting the FE electronics and the light source to the electronics rack are also run and connected at this

Table 1.10: CISC system interface links

Interfacing System	Description	Linked Reference
APA	static T-gradient monitors, cameras, and lights	DocDB 6679 [23]
PD system	PrMs, light emitting system for cameras	DocDB 6730 [24]
TPC Electronics	Noise, Power supply monitoring	DocDB 6745 [25]
HV Systems	shielding, bubble generation by inspection camera, cold camera locations, ground planes	DocDB 6787 [26]
DAQ	Description of CISC data storage, allowing bi-directional communications between DAQ and CISC.	DocDB 6790 [27]
Calibration	multifunctional CISC/CITF ports; space sharing around ports	DocDB 7072 [28]
Physics	Indirect interfaces through calibration, tools to extract data from the slow controls database	DocDB 7099 [29]
Software & Computing	Slow Controls database design and maintenance	DocDB 7126 [30]
Cryogenics	must be designed and implemented. purity monitors, gas analyzers, interlock mechanisms to prevent contamination of LAr	-
Beam	beam status	-
TC Facility	Significant interfaces at multiple levels	DocDB 6991 [31]
TC Installation	Significant interfaces at multiple levels	DocDB 7018 [32]
TC Integration Facility	Significant interfaces at multiple levels	DocDB 7045 [33]

time. This allows the system to be turned on and the software to begin testing the various components and connections. Once all connections are confirmed successful, integration with the slow controls system begins, first by establishing communication between the two systems and then transferring data between them to ensure successful exchange of important system parameters and measurements.

Commissioning the purity monitor system begins once the cryostat is purged and a gaseous argon atmosphere is present. At this time, the HV for the purity monitors is ramped up without risk of discharge through the air, and the light source turned on. Although the drift electron lifetime in the gaseous argon would be very large and therefore not measurable with the purity monitors themselves, the signal strength at both the cathode and anode will give a good indication of how well the light source generates drift electrons from the photocathode. Comparing the signal strengths at the anode and cathode will indicate whether the electrons successfully drift to the anode. Although quality assurance (QA) and quality control (QC) should make it unlikely for a purity monitor to fail this final test, if that does happen then the electric and optical connections can be fixed before filling.

1.4.5.2 Thermometers

Static T-gradient monitors must be installed before the outer APAs, ideally right after the pipes are installed. The profilers are preassembled before they are delivered to SURF. Installation will follow these steps:

1. anchor the stainless steel bottom plates to the four bolts on the bottom corner of the cryostat,
2. anchor the stainless steel support holding the two strings to the four bolts on the top corner of the cryostat,
3. unroll the array with the help of the scissor lift,
4. anchor the strings to the bottom stainless steel support,
5. check and adjust tension and verticality,
6. review all cable and sensor supports,
7. route cable from the top anchoring point to the two DSS ports, and
8. plan to plug sensors into IDC-4 connectors later, just before moving the corresponding APA into its final position.

Individual temperature sensors on pipes and cryostat floor are installed immediately after installing the static T-gradient monitors. First, vertical stainless steel strings for cable routing are installed following a procedure similar to the one described above for the static T-gradient monitors. Next, we anchor all cable supports to pipes. Then each cable is routed individually starting from the

sensor end (with IDC-4 female connector but without the sensor) to the corresponding cryostat port. Once all cables going through the same port have been routed, we cut the cables to the same length, so they can be properly assembled into the corresponding connector(s). To avoid damaging the sensors, they are installed later (by plugging the IDC-4 male connector on the sensor PCB to the IDC-4 female connector on the cable end), just before unfolding the bottom GPs.

For the SP, individual sensors on the top GP must be integrated with the GPs. For each CPA (with its corresponding four GP modules) going inside the cryostat, cable and sensor supports will be anchored to the GP threaded rods as soon as possible. Once the CPA is moved into its final position and its top GPs are ready to be unfolded, sensors on these GPs are installed. Once unfolded, cables exceeding the GP limits can be routed to the corresponding cryostat port using either neighboring GPs or DSS I-beams.

Dynamic T-gradient monitors are installed after the TPC components are in place. Figure 1.8 shows the design of the dynamic T-gradient monitor with its sensor carrier rod, enclosure above the cryostat, and stepper motor and Figure 1.9 shows detailed views of key components. Each monitor comes in several segments with sensors and cabling already in place. Additional slack will be provided at segment joints to make installation easier. Segments of the sensor carrier rod with preattached sensors are fed into the flange one at a time. Each segment, as it is fed into the cryostat, is held at the top with a pin that prevents the segment from sliding all the way in. The next segment is connected at that time to the previous segment. Then the pin is removed, the first segment is pushed down, and the next segment top is held with the pin at the flange. This process is repeated for each segment until the entire sensor carrier rod is in place. Next, the enclosure is installed on top of the flange, starting with the six-way cross at the bottom of the enclosure. (See Figure 1.9, right.) Again, extra cable slack at the top will be provided to ease connection to the D-sub flange and to allow the entire system to move vertically. The wires are connected to a D-sub connector on the feedthrough on one side port of the cross. Finally, a crane positions the remainder of the enclosure above the top of the cross. This enclosure includes the mechanism used to move the sensor rod, which is preassembled with the motor in place on the side of the enclosure, and the pinion and gear used to move the sensor inside the enclosure. The pinion gets connected to the top of the rod. The enclosure is then connected to top part of the cross, which finishes the installation of the dynamic T-gradient monitor.

Commissioning all thermometers will occur in several steps. In the first stage, only cables are installed, so the readout performance and the noise level inside the cryostat is tested with precision resistors. Once sensors are installed, the entire chain is checked again at room temperature. Spare cables, connectors and sensors are available for replacement at Sanford Underground Research Facility (SURF) if needed. The final commissioning phase takes place during and after cryostat filling.

1.4.5.3 Gas Analyzers

The gas analyzers are installed before the piston purge and gas recirculation phases of the cryostat commissioning. They are installed near the tubing switchyard to minimize tubing run length and for convenience when switching the sampling points and gas analyzers. Because each is a

standalone module, a single rack with shelves is adequate to house the modules.

For integration, the gas analyzers typically have an analog output (4 mA to 20 mA or 0 V to 10 V), which maps to the input range of the analyzers. They also usually have several relays to indicate the scale they are currently running. These outputs can be connected to the slow controls for readout. However, using a digital readout is preferable because this gives a direct analyzer reading at any scale. Currently, the digital output connections are RS-232, RS-485, USB, and Ethernet. The preferred option is chosen at the time of purchase. The readout usually responds to a simple set of text query commands. Because of the natural time scales of the gas analyzers and lags in gas delivery times (which depend on the length of the tubing run), sampling every minute is adequate. Our current plan is to record both analog and digital signals to have both outputs available.

The analyzers must be brought online and calibrated before beginning the gas phase of the cryostat commissioning. Calibration varies by module because they are different, but calibration often requires using argon gas with zero contaminants, and argon gas with a known level of the contaminant to check the scale. Contaminants are usually removed with a local inline filter for the first gas sample. This gas phase usually begins with normal air, with the more sensitive analyzers valved off at the switchyard to prevent overloading their inputs (and potentially saturating their detectors). As the argon purge and gas recirculation progress, the various analyzers are valved back in when the contaminant levels reach the upper limits of the analyzer ranges.

1.4.5.4 Liquid Level Monitoring

Installing differential pressure level meters is the responsibility of LBNF, but the capacitive level meters fall within CISC's scope. The exact number of capacitive level meters must still be decided. There will be at least four, located at the four corners of the cryostat. They will be attached to the M10 bolts in the cryostat corners after the detector is installed. Cables will be routed to the appropriate DSS port. If additional capacitive level meters are needed in the central part of the cryostat, those will be installed before the nearby APAs.

1.4.5.5 Pressure Meters

Installing pressure meters is the responsibility of CISC. A total of six sensors will be mechanically installed in two dedicated flanges (three sensors each) at opposite sides of the cryostat after the detector is installed. Cables will be routed through the same dedicated port assigned for these devices. The pressure signals (absolute and relative) are read and converted to standard 4–20 mA current loop signals. A twisted pair shielded cable connects the sensors to the slow controls PLC controller using software to convert electrical signals to pressure values.

1.4.5.6 Cameras and light emitting system

Installing fixed cameras is, in principle, simple but involves a considerable number of interfaces. The enclosure of each camera has exterior threaded holes to facilitate mounting on the cryostat wall, cryogenic internal piping, or DSS. Each enclosure is attached to a gas line to maintain appropriate underpressure in the fill gas, therefore an interface with cryogenic internal piping will be necessary. Each camera has a cable (coaxial or optical) for the video signal and a multiconductor cable for power and control. These get run through cable trays to flanges on assigned instrumentation feedthroughs.

The inspection camera is designed to be inserted and removed on any instrumentation feedthrough equipped with a gate valve at any time during operation. Installing the gate valves and purge system for instrumentation feedthroughs falls under cryogenic internal piping.

Installing fixed lighting sources separate from the cameras requires mounting on cryostat wall, cryogenic internal piping, or DSS, and multiconductor cables for power run through cable trays to flanges on assigned instrumentation feedthroughs.

1.4.5.7 Slow Controls Hardware

Slow controls hardware installation includes installing multiple servers, network cables, any specialized cables needed for device communication, and possibly some custom-built hardware to monitor racks. The installation sequence will be planned with the facilities group and other consortia. The network cables and rack monitoring hardware will be common across many racks and will be installed first as part of the basic rack installation, to be led by the facilities group. Specialized cables needed for slow controls and servers are installed after the common rack hardware. The selection and installation of these cables will be coordinated with other consortia, and servers will be coordinated with the DAQ group.

1.4.5.8 Transport, handling, and storage

Most instrumentation devices will be shipped in pieces to SURF via the South Dakota Warehouse Facility (SDWF) and mounted on-site. Instrumentation devices are in general small, except for the support structures for purity monitors and dynamic T-gradient monitors, which will cover the entire height of the cryostat. The load on those structures is relatively small ($< 100\,\mathrm{kg}$), so they can be fabricated in sections of less than 3 m, which can be easily transported to SURF, down the shaft, and through the tunnels. All instrumention devices except the dynamic T-gradient monitors can be moved into the cryostat without the crane. The dynamic T-gradient monitors, which are introduced into the cryostat from above, require a crane for the installation of the external enclosure (with preassembled motor, pinion and gear).

1.4.6 Quality Control

The manufacturer and the institution in charge of device assembly will conduct a series of tests to ensure the equipment can perform its intended function as part of QC. QC also includes post-fabrication tests and tests run after shipping and installation. For complex systems, the entire system will be tested before shipping. Additional QC procedures can be performed underground after installation.

The planned tests for each subsystem are described below.

1.4.6.1 Purity Monitors

The purity monitor system will undergo a series of tests to ensure the system performs as intended. These tests reflect the ProtoDUNE-SP purity monitor QC tests, which included electronic tests with a pulse generator, mechanical and electrical connectivity tests at cryogenic temperatures in a cryostat, and vacuum tests for short and full assemblies in a dewar and in a long vacuum tube.

The QC tests for FD purity monitors begin with testing individual purity monitors in vacuum after each is fabricated and assembled. This test checks the amplitude of the signal generated by the drift electrons at the cathode and the anode to ensure the photocathode can provide sufficient numbers of photoelectrons to measure the signal attenuation with the required precision, and that the field gradient resistors all work properly to maintain the drift field. A smaller version of the assembly with all purity monitors installed will be tested at the CITF to ensure the full system performs as expected in LAr.

Next, the entire system is assembled on the full-length mounting tubes to check the connections along the way. Ensuring that all electric and optical connections are operating properly during this test reduces the risk of problems once the full system is assembled and ready for the final test in vacuum. The fully assembled system is placed in the shipping tube, which serves as a vacuum chamber, and tested at SURF before the system is inserted into the cryostat. During insertion, electrical connections are tested continuously with multimeters and electrometers.

1.4.6.2 Thermometers

Static T-gradient thermometers Static T-gradient monitors undergo three type of tests at the production site before shipment to SURF: a mechanical rigidity test, a calibration of all sensors, and a test of all electrical cables and connectors. The mechanical rigidity is tested by mounting the static T-gradient monitor between two dummy cryostat corners mounted 15 m apart. The tension of the strings is set to match the tension that would occur in a vertical deployment in LAr, and the deflection of the sensor and electrical cable strings is measured and compared to the expected value; this is to ensure any swinging or deflection of the deployed static T-gradient monitor will be < 5 cm, mitigating any risk of touching the anode plane assemblies. The laboratory calibration of sensors will be performed as explained in Section 1.2.1. The main concern is reproducibility of

results because sensors could change resistance and hence their temperature scale when undergoing successive immersions in LAr. In this case, the calibration procedure itself provides QC because each set of sensors goes through five independent measurements. Sensors with RMS variation outside the requirement (2 mK for ProtoDUNE-SP) are discarded. This calibration also serves as QC for the readout system (similar to the final one) and of the PCB-sensor-connector assembly. Finally, the cable-connector assemblies are tested; sensors must measure the expected values with no additional noise introduced by either cable or connector.

An integrated system test is conducted at a LAr test facility at the production site, which has sufficient linear dimension (>2 m) to test a good portion of the system. This ensures that the system operates in LAr at the required level of performance. The laboratory sensor calibration is compared with the in situ calibration of the dynamic T-gradient monitors by operating both dynamic and static T-gradient monitors simultaneously.

The last phase of QC takes place after installation. The verticality of each array is checked, and the tensions in the stainless steel strings adjusted as necessary. Before closing the flange, the entire readout chain is tested. This allows a test of the sensor-connector assembly, the cable-connector assemblies at both ends, and the noise level inside the cryostat. If any sensor presents a problem, it is replaced. If the problem persists, the cable is checked and replaced as needed.

Dynamic T-gradient thermometers The dynamic T-gradient monitor consists of an array of high-precision temperature sensors mounted on a vertical rod. The rod can move vertically to cross-calibrate the temperature sensors in situ. We will use the following tests to ensure that the dynamic T-gradient monitor delivers vertical temperature gradient measurements with a precision of a few mK.

- Before installation, temperature sensors are tested in LN to verify correct operation and to set the baseline calibration for each sensor with respect to the absolutely calibrated reference sensor.
- Warm and cold temperature readings are taken with each sensor after it is mounted on the PCB board and the readout cables are soldered
- The sensor readout is taken for all sensors after the cold cables are connected to electric feedthroughs on the flange and the warm cables outside of the cryostat are connected to the temperature readout system.
- The stepper motor is tested before and after connecting to the gear and pinion system.
- The fully assembled rod is connected to the pinion and gear and moved with the stepper motor on a high platform many times to verify repeatability, possible offsets, and any uncertainty in the positioning. Finally, repeating this test so many times will verify the sturdiness of the system.
- The full system is tested after it is installed in the cryostat; both motion and sensor operation are tested by checking sensor readout and vertical motion of the system.

Individual Sensors To address the quality of individual precision sensors, the same method as for the static T-gradient monitors is used. The QC of the sensors is part of the laboratory calibration. After mounting six sensors with their corresponding cables, a SUBD-25 connector is added, and the six sensors tested at room temperature. All sensors must give values within specifications. If any of the sensors present problems, they are replaced. If the problem persists, the cable is checked and replaced as needed.

For standard RTDs to be installed on the cryostat walls, floor, and roof, calibration is not an issue. Any QC required for associated cables and connectors is performed following the same procedure as for precision sensors.

1.4.6.3 Gas Analyzers

The gas analyzers will be guaranteed by the manufacturer. However, once received, the gas analyzer modules are checked for both *zero* and the *span* values using a gas-mixing instrument and two gas cylinders, one having a zero level of the gas analyzer contaminant species and the other cylinder with a known percentage of the contaminant gas. This verifies the proper operation of the gas analyzers. When they are installed at SURF, this process is repeated before commissioning the cryostat. Calibrations will need to be repeated per manufacturer recommendations over the gas analyzer lifetime.

1.4.6.4 Liquid Level Monitoring

The manufacturer will provide the QC for the differential pressure level meters; further QC during and after installation is the responsibility of LBNF.

The capacitive sensors will be tested with a modest sample of LAr in the laboratory before they are installed. After installation, they are tested in situ using a suitable dielectric in contact with the sensor.

1.4.6.5 Pressure Meters

The manufacturer will provide the QC for the pressure meters; further QC during and after installation is the responsibility of CISC.

The pressure sensors will be tested with a modest sample of gaseous argon in the laboratory before they are installed. After installation, they are tested in situ at atmospheric pressure. The whole pressure readout chain, (including slow controls PLC and WINCC conversion) will also be tested and cross-checked with LBNF pressure sensors.

1.4.6.6 Cameras

Before transport to SURF, each cryogenic camera unit (comprising the enclosure, camera, and internal thermal control and monitoring) is checked for correct operation of all features, for recovery from 87 K non-operating mode, for leakage, and for physical defects. Lighting systems are similarly checked. Operations tests will verify correct current draw, image quality, and temperature readback and control. The movable inspection camera apparatus are inspected for physical defects and checked for proper mechanical operation before shipping. A checklist is created for each unit, filed electronically in the DUNE logbook, and a hard copy sent with each unit.

Before installation, each fixed cryogenic camera unit is inspected for physical damage or defects and checked at the CITF for correct operation of all features, for recovery from 87 K non-operating mode, and for contamination of the LAr. Lighting systems are similarly checked. Operations tests verify correct current draw, image quality, and temperature readback and control. After installation and connection of wiring, fixed cameras and lighting are again checked for operation. The movable inspection camera apparatus is inspected for physical defects and, after integration with a camera unit, tested in the facility for proper mechanical and electronic operation and cleanliness before being installed or stored. A checklist will be completed for each QC check and filed electronically in the DUNE logbook.

1.4.6.7 Light-emitting System

The entire light-emitting system is checked before installation to ensure functionality of light emission. Initial testing of the system (see Figure 1.29) begins with measuring the current when low voltage (1 V) is applied, to check that the resistive LED failover path is correct. Next, the forward voltage is measured using nominal forward current to check that it is within 10 % of the nominal forward voltage drop of the LED, that all of the LEDs are illuminated, and that each LED is visible over the nominal angular range. If the LEDs are infrared, a video camera with the IR filter removed is used for a visual check. This procedure is then duplicated with the current reversed for LEDs oriented in the opposite direction. Initial tests are performed at room temperature and then repeated in LN. Color shifts in the LEDs are expected and will be noted. A checklist is completed for each QC check and filed electronically in the DUNE logbook.

Room temperature tests are repeated during and immediately after installation to ensure that the system has not been damaged during transportation or installation. Functionality checks of the LEDs are repeated after the cameras are installed in the cryostat.

1.4.6.8 Slow Controls Hardware

Networking and computing systems will be purchased commercially, requiring manufacturer's QA. However, the new servers are tested after delivery to confirm they suffered no damage during shipping. The new system is allowed to burn in overnight or for a few days, running a diagnostics suite on a loop in order to validate the manufacturer's QA process.

The system is shipped directly to SURF where an on-site expert boots the systems and does basic configuration. Specific configuration information is pulled over the network, after which others may log in remotely to do the final setup, minimizing the number of people underground.

1.4.7 Safety

Safety is of critical importance during all phases of the CISC project, including R&D, laboratory calibration and testing, mounting tests, and installation. Safety experts review and approve the initial safety planning for all phases as part of the initial design review, as well as before implementation. All documentation of component cleaning, assembly, testing, and installation will include a section on relevant safety concerns and will be reviewed during appropriate pre-production reviews.

Several areas are of particular importance to CISC.

- Hazardous chemicals (e.g., epoxy compounds used to attach sensors to cryostat inner membrane) and cleaning compounds: All chemicals used will be documented at the consortium management level, with a MSDS (material safety data sheet) and approved handling and disposal plans in place.
- Liquid and gaseous cryogens used in calibrating and testing: LN and LAr are used to calibrate and test instrumentation devices. Full hazard analysis plans will be in place at the consortium management level for full module or module component testing that involves cryogens. These safety plans will be reviewed in appropriate pre-production and production reviews.
- High voltage safety: Purity monitors have a voltage of $\sim 2\,\mathrm{kV}$. Fabrication and testing plans will show compliance with local HV safety requirements at any institution or laboratory that conducts testing or operation, and this compliance will be reviewed as part of the standard review process.
- Working at heights: Some fabrication, testing, and installation of CISC devices require working at heights. Both T-gradient monitors and purity monitors, which span the height of the detector, require working at heights exceeding 10 m. Temperature sensors installed near the top cryostat membrane and cable routing for all instrumentation devices also require working at heights. The appropriate safety procedures including lift and harness training will be designed and reviewed.
- Falling objects: all work involving heights have associated risks of falling objects. The corresponding safety procedures, including proper helmet use and a well restricted safety area, will be included in the safety plan.

Glossary

Fermi National Accelerator Laboratory (Fermilab) U.S. national laboratory in Batavia, IL. It is the laboratory that hosts Deep Underground Neutrino Experiment (DUNE) and serves as its near site. 68

MicroBooNE The LArTPC-based MicroBooNE neutrino oscillation experiment at Fermi National Accelerator Laboratory (Fermilab). 45

NOvA The NOvA off-axis neutrino oscillation experiment at Fermilab. 45

35 ton prototype A prototype cryostat and single-phase (SP) detector built at Fermilab before the ProtoDUNE detectors. 16, 27, 30, 35–37

anode plane assembly (APA) A unit of the SP detector module containing the elements sensitive to ionization in the LAr. It contains two faces each of three planes of wires, and interfaces to the cold electronics and photon detection system. 1, 3, 11, 19, 38, 39, 47, 54, 58, 59, 61, 63

American wire gauge (AWG) U.S. standard set of non-ferrous wire conductor sizes. 16

cold electronics (CE) Analog and digital readout electronics that operate at cryogenic temperatures. 42

European Organization for Nuclear Research (CERN) The leading particle physics laboratory in Europe and home to the ProtoDUNEs. (In French, the Organisation Européenne pour la Recherche Nucléaire, derived from Conseil Européen pour la Recherche Nucléaire. 48, 71, 72

conventional facilities (CF) Pertaining to construction and operation of buildings and conventional infrastructure, and for LBNF and DUNE project (LBNF/DUNE), CF includes the excavation caverns. 70

computational fluid dynamics (CFD) High performance computer-assisted modeling of fluid dynamical systems. 4, 6, 10–14, 22, 24–27, 33, 48, 50, 52

cryogenic instrumentation and slow controls (CISC) Includes equipment to monitor all detec-

tor components and liquid argon (LAr) quality and behavior, and provides a control system for many of the detector components. 1–6, 13, 32, 41–46, 50–54, 56–58, 61, 65, 67

cryogenic instrumentation test facility (CITF) A facility at Fermilab with small ($<$ 1 ton) to intermediate ($\sim$ 1 ton) volumes of instrumented, purified TPC-grade LAr, used for testing devices intended for use in DUNE. 4, 6, 9, 32, 38, 40, 41, 48, 52, 55, 58, 63, 66

cathode plane assembly (CPA) The component of the SP detector module that provides the drift HV cathode. 38, 39

charge-parity symmetry violation (CPV) Lack of symmetry in a system before and after charge and parity transformations are applied. 1

charge-readout plane (CRP) In the dual-phase (DP) technology, a collection of electrodes in a planar arrangement placed at a particular voltage relative to some applied E field such that drifting electrons may be collected and their number and time may be measured. 36–39, 47

central utility cavern (CUC) The utility cavern at the 4850L of Sanford Underground Research Facility (SURF) located between the two detector caverns. It contains utilities such as central cryogenics and other systems, and the underground data center and control room. 43, 44, 53

data acquisition (DAQ) The data acquisition system accepts data from the detector front-end (FE) electronics, buffers the data, performs a trigger decision, builds events from the selected data and delivers the result to the offline secondary DAQ buffer. 5, 30–32, 44–47, 50, 58, 62, 70

DUNE detector safety system (DDSS) The system used to manage key aspects of detector safety. 5

detector module The entire DUNE far detector is segmented into four modules, each with a nominal 10 kt fiducial mass. 3, 4, 6, 9–11, 13, 14, 16, 20, 22, 26, 27, 32, 33, 36, 37, 41, 46, 50, 53, 69, 72

dual-phase (DP) Distinguishes one of the DUNE far detector technologies by the fact that it operates using argon in both gas and liquid phases. 1, 10, 11, 33, 69, 71, 72

DP module dual-phase DUNE far detector (FD) module. 1, 50

detector support system (DSS) The system used to support a SP detector module within its cryostat. 14, 20, 22, 59, 61, 62

Deep Underground Neutrino Experiment (DUNE) A leading-edge, international experiment for neutrino science and proton decay studies. 9–11, 26, 35, 37, 38, 42, 48, 56, 66, 68–70, 72

field cage (FC) The component of a liquid argon time-projection chamber (LArTPC) that contains and shapes the applied E field. 3, 10, 38, 39

far detector (FD) The 40 kt fiducial mass DUNE detector, composed of four 10 kt modules, to be installed at the far site at SURF in Lead, SD, USA. 1, 3, 11, 33, 34, 38, 41, 42, 45, 46, 50, 52, 54, 63, 69, 70, 72

front-end (FE) The front-end refers a point that is "upstream" of the data flow for a particular subsystem. For example the front-end electronics is where the cold electronics meet the sense wires of the TPC and the front-end data acquisition (DAQ) is where the DAQ meets the output of the electronics. 30, 32, 44, 57, 69

far site conventional facilities (FSCF) The conventional facilities (CF) at the DUNE far detector site, SURF. 72

ground plane (GP) An electrode that is held to be electrically neutral relative to Earth ground voltage. 6, 10, 20, 22, 33, 37, 38, 60

high voltage (HV) Generally describes a voltage applied to drive the motion of free electrons through some media, e.g., LAr. 3, 5, 6, 25, 29–33, 36, 37, 39, 42, 47, 54, 57–59, 67

IFbeam Database that stores beamline information indexed by timestamp. 46, 47

IFIC Instituto de Fisica Corpuscular (in Valencia, Spain). 20

liquid argon (LAr) Argon in its liquid phase; it is a cryogenic liquid with a boiling point of −90 °C (87 K) and density of 1.4 g/ml. 1, 3–6, 10–14, 19, 22–27, 29, 32, 33, 35–42, 50, 54, 55, 63–67, 69, 70, 72

liquid argon time-projection chamber (LArTPC) A time projection chamber (TPC) filled with liquid argon; the basis for the DUNE FD modules. 27, 32, 69

Long-Baseline Neutrino Facility (LBNF) The organizational entity responsible for developing the neutrino beam, the cryostats and cryogenics systems, and the conventional facilities for DUNE. 4, 33, 34, 46, 50, 52, 54, 56, 57, 61, 65, 72

LBNF and DUNE project (LBNF/DUNE) The overall global project, including Long-Baseline Neutrino Facility (LBNF) and DUNE. 68

LED Light-emitting diode. 41, 66

LHC Large Hadron Collider. 48

LN liquid nitrogen. 41

LV low voltage. 32

Proton Assembly Building (PAB) Home of several LAr facilities at Fermilab. 41, 42

photon detector (PD) The detector elements involved in measurement of the number and arrival times of optical photons produced in a detector module. 3, 42, 47

photon detection system (PD system) The detector subsystem sensitive to light produced in the LAr. 32, 41, 58

PLC programmable logic controller. 61

parts per billion (ppb) A concentration equal to one part in 10^{-9}. 26

parts per trillion (ppt) A concentration equal to one part in 10^{-12}. 26

ProtoDUNE Either of the two DUNE prototype detectors constructed at European Organization for Nuclear Research (CERN). One prototype implements SP technology and the other DP. 12, 32–34, 38, 43, 48, 50, 52, 54, 55, 68, 71

ProtoDUNE-2 The second run of a ProtoDUNE detector. 52, 53

ProtoDUNE-DP The DP ProtoDUNE detector at CERN. 3, 10, 27, 33, 38, 42, 48, 53

ProtoDUNE-SP The SP ProtoDUNE detector at CERN. 3, 5, 6, 8, 10–14, 16, 18–20, 22, 23, 25–30, 32–34, 37–42, 45, 46, 48, 49, 52–54, 63, 64

production readiness review (PRR) A project management device by which the production readiness is reviewed. 53

quality assurance (QA) The set of actions taken to provide confidence that quality requirements are fulfilled, and to detect and correct poor results. 59, 66

quality control (QC) An aggregate of activities (such as design analysis and inspection for defects) performed to ensure adequate quality in manufactured products. 59, 63–66

risk probabilities The risk probability, after taking into account the planned mitigation activities, is ranked as L (low, $<10\,\%$), M (medium, $10\,\%$ to $25\,\%$), or H (high, $>25\,\%$). The cost and schedule impacts are ranked as L (cost increase$<5\,\%$, schedule delay <2 months), M ($5\,\%$ to $25\,\%$ and 2–6 months, respectively) and H ($>20\,\%$ and >2 months, respectively). 55

Resistance temperature detector (RTD) A temperature sensor consisting of a material with an accurate and reproducible resistance/temperature relationship. 32

signal-to-noise (S/N) signal-to-noise ratio. 3

SCADA supervisory control and data acquisition. 48

South Dakota Warehouse Facility (SDWF) Warehousing operations in South Dakota responsible for receiving LBNF and DUNE goods and coordinating shipping to the Ross Shaft at SURF. 62

secondary DAQ buffer A secondary DAQ buffer holds a small subset of the full rate as selected by a trigger command. This buffer also marks the interface with the DUNE Offline. 69

silicon photomultiplier (SiPM) A solid-state avalanche photodiode sensitive to single photoelectron signals. 1

supernova neutrino burst (SNB) A prompt increase in the flux of low-energy neutrinos emitted in the first few seconds of a core-collapse supernova. It can also refer to a trigger command type that may be due to this phenomenon, or detector conditions that mimic its interaction signature. 1

single-phase (SP) Distinguishes one of the DUNE far detector technologies by the fact that it operates using argon in its liquid phase only. 1, 6, 11, 33, 42, 60, 68, 69, 71

SP module single-phase DUNE FD module. 4, 12, 14, 19, 26, 29, 32, 33, 42, 48, 50, 54

Sanford Underground Research Facility (SURF) The laboratory in South Dakota where the LBNF far site conventional facilities (FSCF) will be constructed and the DUNE FD will be installed and operated. 60, 69, 72

technical design report (TDR) A formal project document that describes the experiment at a technical level. 1

time projection chamber (TPC) A type of particle detector that uses an E field together with a sensitive volume of gas or liquid, e.g., LAr, to perform a 3D reconstruction of a particle trajectory or interaction. The activity is recorded by digitizing the waveforms of current induced on the anode as the distribution of ionization charge passes by or is collected on the electrode. 1, 3, 6, 9, 12, 14, 27, 32, 36, 37, 41, 42, 47, 53, 54, 58, 60, 70

trigger candidate Summary information derived from the full data stream and representing a contribution toward forming a trigger decision. 72

trigger command Information derived from one or more trigger candidates that directs elements of the detector module to read out a portion of the data stream. 72

trigger decision The process by which trigger candidates are converted into trigger commands. 69, 72

WA105 DP demonstrator The $3 \times 1 \times 1\,\mathrm{m}^3$ WA105 DP prototype detector at CERN. 36

wavelength-shifting (WLS) A material or process by which incident photons are absorbed by a material and photons are emitted at a different, typically longer, wavelength. 73

X-ARAPUCA ARAPUCA design with wavelength-shifting (WLS) coating on only the external face of the dichroic filter window(s) but with a WLS doped plate inside the cell. 3

References

[1] DOE Office of High Energy Physics, "Mission Need Statement for a Long-Baseline Neutrino Experiment (LBNE)," tech. rep., DOE, 2009. LBNE-doc-6259.

[2] G. J. Michna *et al.*, "CFD Analysis of Fluid, Heat, and Impurity Flows in DUNE FAR Detector to Address Additional Design Considerations," DUNE doc 5915, South Dakota State University, 2017. https://docs.dunescience.org/cgi-bin/private/ShowDocument?docid=5915&asof=2019-7-15.

[3] Strons, Ph., and Bailey, J. L., "Flow visualization methods for field test verification of CFD analysis of an ope n gloveport," 2017. https://www.osti.gov/pages/servlets/purl/1402050.

[4] The Liquid Argon Technology @BNL, "Basic properties." https://lar.bnl.gov/properties/basic.html. Accessed Jan. 15, 2019.

[5] A. Kehrli, G. L. Miotto, X. Pons, S. Ravat, and M. J. Rodriguez, "The protoDUNE Single Phase Detector Control System, in Proceedings of CHEP 2018," tech. rep., 2018. https://docs.dunescience.org/cgi-bin/private/ShowDocument?docid=11098.

[6] W. Walkowiak, "Drift velocity of free electrons in liquid argon," *Nucl. Instrum. Meth.* **A449** (2000) 288–294.

[7] L. Whitehead, "DUNE Far Detector Task Force Final Report," DUNE doc 3384, 2018. https://docs.dunescience.org/cgi-bin/private/ShowDocument?docid=3384&asof=2019-7-15.

[8] M. Adamowski *et al.*, "The Liquid Argon Purity Demonstrator," *JINST* **9** (2014) P07005, arXiv:1403.7236 [physics.ins-det].

[9] **WA105** Collaboration, S. Murphy, "Status of the WA105-3x1x1 m^3 dual phase prototype," tech. rep., 2017. https://indico.fnal.gov/event/12345/session/1/contribution/5/material/slides/0.pdf.

[10] Delaquis, S. C. and Gornea, R. and Janos, S. and Lüthi, M. and Rudolf von Rohr, C. and Schenk, M. and Vuilleumier, J. -L., "Development of a camera casing suited for cryogenic

and vacuum applications," *JINST* **8** (2013) T12001, arXiv:1310.6601 [physics.ins-det].

[11] Auger, M. and Blatter, A. and Ereditato, A. and Goeldi, D. and Janos, S. and Kreslo, I. and Lüthi, M. and Rudolf von Rohr, C. and Strauss, T. and Weber, M. S., "On the Electric Breakdown in Liquid Argon at Centimeter Scale," *JINST* **11** no. 03, (2016) P03017, arXiv:1512.05968 [physics.ins-det].

[12] T. I. Banks *et al.*, "A compact ultra-clean system for deploying radioactive sources inside the KamLAND detector," *Nucl. Instrum. Meth.* **A769** (2015) 88–96, arXiv:1407.0413 [physics.ins-det].

[13] "LUXEON C Color Line (datasheet)." https://www.lumileds.com/uploads/571/DS144-pdf. Accessed: 2018-11-19.

[14] J. Carron, A. Philippon, L. S. How, A. Delbergue, S. Hassanzadeh, D. Cillierre, P. Danto, and M. Boutillier, "Cryogenic characterization of LEDs for space application," *Proc. SPIE, Sixteenth International Conference on Solid State Lighting and LED-based Illumination Systems* **10378** (2017) 20.

[15] Siemens AG, "SIMATIC WinCC open architecture." http:///www.siemens.com/wincc-open-architecture. Accessed: 2018-11-27.

[16] "EPICS - Experimental Physics and Industrial Control System." https://epics-controls.org/. Accessed: July 19, 2019.

[17] R. Acciarri *et al.*, "Design and construction of the microboone detector," *Journal of Instrumentation* **12** no. 02, (2017) P02017. http://stacks.iop.org/1748-0221/12/i=02/a=P02017.

[18] G. Lukhanin, K. Biery, S. Foulkes, M. Frank, A. Hatzikoutelis, J. Kowalkowski, M. Paterno, and R. Rechenmacher, "Application of control system studio for the NOvA detector control system," *J. Phys. Conf. Ser.* **396** (2012) 062012.

[19] "About JCOP." http://jcop.web.cern.ch/. Accessed: July 19, 2019.

[20] "UNICOS," 2015. http://unicos.web.cern.ch/.

[21] A. C. Villanueva and S. Gollapinni, "DUNE FD WBS: Slow Control," DUNE doc 5609, 2018. https://docs.dunescience.org/cgi-bin/private/ShowDocument?docid=5609&asof=2019-7-15.

[22] S. Gollapinni *et al.*, "DUNE FD Risks: CISC,". https://docs.dunescience.org/cgi-bin/private/ShowDocument?docid=7192&asof=2019-7-15.

[23] A. C. Villanueva *et al.*, "DUNE FD Interface Document for Single Phase/Joint: SP APA to Joint CISC,". https://docs.dunescience.org/cgi-bin/private/ShowDocument?docid=6679&version=1.

[24] A. C. Villanueva *et al.*, "DUNE FD Interface Document: SP Photon Detector to Joint CISC," DUNE doc 6730, 2018. https://docs.dunescience.org/cgi-bin/private/ShowDocument?docid=6730&asof=2019-7-15.

[25] A. Cervera Villanueva, D. Christian, S. Gollapinni, and M. Verzocchi, "DUNE Interface Document: CISC / SP–TPC Cold Electronics," DUNE doc 6745, 2018. https://docs.dunescience.org/cgi-bin/private/ShowDocument?docid=6745&asof=2019-7-15.

[26] A. C. Villanueva *et al.*, "DUNE FD Interface Document: High Voltage to CISC,". https://docs.dunescience.org/cgi-bin/private/ShowDocument?docid=6787&version=1.

[27] A. C. Villanueva *et al.*, "DUNE FD Interface Document: DAQ to CISC,". https://docs.dunescience.org/cgi-bin/private/ShowDocument?docid=6790&version=1.

[28] S. Gollapinni *et al.*, "DUNE FD Interface Document: Calibration to Joint CISC,". https://docs.dunescience.org/cgi-bin/private/ShowDocument?docid=7072&version=1.

[29] S. Gollapinni *et al.*, "DUNE FD Interface Document: DUNE Physics to Joint CISC,". https://docs.dunescience.org/cgi-bin/private/ShowDocument?docid=7099&version=1.

[30] S. Gollapinni *et al.*, "DUNE FD Interface Document: Software and Computing to Joint CISC,". https://docs.dunescience.org/cgi-bin/private/ShowDocument?docid=7126&version=1.

[31] F. Feyzi *et al.*, "DUNE FD Interface Document: Facility Interfaces to Joint CISC,". https://docs.dunescience.org/cgi-bin/private/ShowDocument?docid=6991.

[32] S. Gollapinni *et al.*, "DUNE FD Interface Document: Installation Interfaces to Joint CISC,". https://docs.dunescience.org/cgi-bin/private/ShowDocument?docid=7018&version=1.

[33] S. Gollapinni *et al.*, "DUNE FD Interface Document: Integration Facility to Joint CISC,". https://docs.dunescience.org/cgi-bin/private/ShowDocument?docid=7045&version=1.